https://doi.org/10.5194/essd-2026-211
Preprint. Discussion started: 27 April 2026

Open Access Earth System Science Data Discussions

Characterization and applications of multi-decadal black carbon observations at a Mediterranean mountain site

Marco Zanatta[1], Paolo Bonasoni[1], Francescopiero Calzolari[1], Paolo Cristofanelli[1], Sabine Eckhardt[2], Nikolaos Evangeliou[2], Cecilia Magnani[1,3], Camilla Perfetti[1,4], Davide Putero[5], Laura Renzi[1], Franziska Vogel[1], and Angela Marinoni[1]

[1]Institute of Atmospheric Sciences and Climate – National Research Council of Italy, Bologna, Italy
[2]Norwegian Institute for Air Research (NILU), Kjeller, Norway
[3]Ca' Foscari University of Venice, Department of Environmental Sciences, Informatics and Statistics, Via Torino 155, 30172 Venice, Italy
[4]Department of Physics and Astronomy, University of Bologna, Bologna, 40126, Italy
[5]Institute of Atmospheric Sciences and Climate – National Research Council of Italy, Turin, Italy

Correspondence to: Marco Zanatta (m.zanatta@isac.cnr.it)

Abstract. Long-term observations of black carbon (BC) are essential for assessing the effectiveness of air-quality and climate policies and for understanding the potential feedback of climate change. We present an 18-year dataset (2007–2024) of equivalent black carbon (eBC) mass concentration derived from the aerosol absorption coefficient measured at the Monte Cimone WMO/GAW Global Station (CMN, 2165 m a.s.l.), a key high-altitude observatory in the Mediterranean climate-change hotspot. The dataset is accompanied by detailed description of: i) the infrastructural evolution, including instrumentation and sampling system; ii) the definition of quality assurance protocol and data treatment; iii) the definition of the uncertainties. This documentation provides a comprehensive description and quantification of the data reliability over 18 years of measurements, necessary for the scientific valorisation of the dataset. Applications of the dataset demonstrate: i) a statistically significant decline in eBC concentrations over the last two decades ii) a strong linkage between eBC variability and boundary-layer dynamics when combined with ERA5 reanalysis; iii) a variable agreement with FLEXPART simulations across temporal scales, supporting its use for model evaluation. The dataset, openly available through the ITINERIS HUB, provides one of the longest continuous eBC records in the Mediterranean troposphere and represents a valuable resource for climate studies, trend assessments, and multi-station integration within ACTRIS and GAW.

1 Introduction

Black carbon (BC) is a short-lived climate forcer produced by incomplete combustion of fossil fuels and biomass. Because of its strong light absorption, BC is the sole aerosol particle with a positive effective radiative forcing (Szopa et al., 2021); while, being a carrier of toxic and carcinogenic substances, it is a major responsible of health issues (Ali et al., 2021). Hence, BC is

https://doi.org/10.5194/essd-2026-211
Preprint. Discussion started: 27 April 2026

a target of both climate and air quality policies (Pisoni et al., 2025). Overall, long-term observations indicates that concentration of BC has been showing a generalized decrease worldwide (Collaud Coen et al., 2020b), confirming the effectiveness of emission reduction polices. However, long term studies indicates that a decreasing trend for other atmospheric species is not generalizable worldwide, where increasing or decreasing tendencies appears on local and regional scale (Kurokawa and Ohara, 2020; Jin et al., 2023; Itahashi and Uno, 2024). Considering the total aerosol, deviations from a decreasing common trend may be associated with specific processes, which may be comprehensively understood combining long-term observations with numerical modelling. Changes in atmospheric circulation (Pernov et al., 2022), shifts in precipitation patterns (Isokääntä et al., 2022), occurrence of heat waves (Heikkinen et al., 2020) but also economic and demographic growth (Kurokawa and Ohara, 2020) have been associated with perturbations in aerosol particles concentration and properties worldwide. Hence, a diffused and permanent network of harmonized in-situ observations such as those embedded in Aerosol, Clouds and Trace Gases Research Infrastructure (ACTRIS-RI; Laj et al., 2024) and the Global Atmosphere Watch programme of the World Meteorological Organization (WMO/GAW; Laj et al., 2020) allows tracing long-term variability of aerosol particles, while integrated, comprehensive observational frameworks are crucial for linking atmospheric processes, climate impacts, and societal responses (Kulmala et al., 2023).

The current work presents in-situ and long-term observations of eBC acquired at the Monte Cimone WMO/GAW Global Station (CMN, 2165 m a.s.l.) that, integrated in wider framework, can contribute to quantify the effectiveness of emission reduction policies and climate change feedback in the Mediterranean region. CMN is a high-altitude observatory in Southern Europe providing an ideal platform to investigate how local, mesoscale and synoptic processes shape BC variability across daily to decadal scales into the context of a changing Mediterranean climate (MedECC, 2020). The 18-year dataset described in the present work refers to equivalent BC (eBC), which is a mass concentration of BC derived from the aerosol absorption coefficient measured with filter-based absorption photometers (Petzold et al., 2013), namely the multi-angle absorption photometer (MAAP, Petzold and Schönlinner, 2004). The dataset is complemented by extensive description of operative conditions, quality-control procedures (WMO/GAW Report No. 227, 2016), comprehensive metadata, and auxiliary parameters suitable for diverse applications. To illustrate its potential, we combine the eBC measurements with the boundary layer height derived from the ERA5 reanalysis fields and with numerical modelling products such as CAMS and FLEXPART, demonstrating how the dataset can support assessments of meteorological influence on eBC variability, model–observation agreement, and the representativeness of long-term trends. This dataset provides one of the longest continuous records of eBC in the Mediterranean troposphere and is designed to support a broad range of applications from model evaluation to climatic and policy assessment.

2 Characteristics of the Monte Cimone observatory

The dataset presented in the current manuscript was acquired at the “Ottavio Vittori Observatory” on the top of Monte Cimone (2165 m a.s.l.; 44°12’ N, 10°42’ E). The observatory is part of the WMO/GAW Global Station Monte Cimone (CMN), and it

https://doi.org/10.5194/essd-2026-211
Preprint. Discussion started: 27 April 2026

is hosted at the premises of the Centro Aeronautica Militare di Montagna (CAMM) of the Italian Air Force. The National Research Council of Italy (CNR; https://ror.org/04zaypm56), trough the Institute of Atmospheric Sciences and Climate (CNR-ISAC; https://ror.org/00n8ttd98), manages the observatory and supervises the in-situ aerosol and trace gas measurements. CMN belongs to European research infrastructures such as ACTRIS-RI (Aerosol, Clouds, Trace Gases Research Infrastructure), and ICOS-RI (Integrated Carbon Observation System) contributing regularly to the international studies characterizing the climatology of European aerosols (e.g. Andrews et al., 2011; Asmi et al., 2011; Laj et al., 2020; Pandolfi et al., 2018) and gases (e.g. Gaudel et al., 2018; Putero et al., 2023). A full description of the site, and the scientific-educational activities carried out at CMN is provided in Cristofanelli et al. (2018). Concerning the meteorology, seasonal temperature variability at CMN is characterized by cold winter conditions (<0°C) and a progressive warming toward a summer maximum (10-15°C). Dew-point temperatures follow closely the ambient temperature seasonal cycle, indicating favourable conditions for cloud formation all year around. A detailed description of meteorology and cloud presence at CMN in the 2007-2024 period is provided in Section S1. Based on the regional orography, CMN is identified as a station periodically influenced by free-tropospheric and boundary layer conditions (Collaud Coen et al., 2018). Due to its geographical position, the footprint of air mass parcels reaching CMN is regularly influenced by contributions from the continental Europe northward and the Mediterranean basin southward (Henne et al., 2010). Hence, observations at CMN allow studying a wide variety of atmospheric processes at local, regional, and continental scales. For instance, the seasonal cycle of aerosol particles (Mazzini et al., 2025), black carbon (Marinoni et al., 2008) and trace gases (Cristofanelli et al., 2009, 2015) reflects local vertical transport between boundary layer and free troposphere; while regional and continental processes, like heatwaves (Cristofanelli et al., 2007), biomass burning events (Cristofanelli et al., 2013, 2021, 2024) and Saharan dust outbreaks (Duchi et al., 2016; Vogel et al., 2025b) affects episodically the aerosol and gas composition. The long-term observations at CMN allow identifying the impacts of Mediterranean climatic anomalies (MedECC, 2020) and emission reduction policies (Fuzzi et al., 2015) on aerosol particle presence and properties.

3 Instrumental setup

In this section we describe the instrumental setup deployed at CMN for the quantification of BC with a filter-based absorption photometer and the infrastructural evolution between 2007 and 2024.

3.1 Multi angle absorption photometer

The Multi–Angle Absorption Photometer (MAAP, model 5012, Thermo Scientific) is a filter-based absorption photometer that measures aerosol light absorption by simultaneously detecting reflected and transmitted light from particles collected on a filter.An inversion algorithm based on the Mie theory and the two-stream approximation is appliedto retrieve the aerosol absorption coefficient at a single wavelength (670 nm), from which the equivalent BC (eBC) mass concentration is derived. More detail on the MAAP operating principle and uncertainties are provided by Petzold and Schönlinner (2004) and Petzold

https://doi.org/10.5194/essd-2026-211
Preprint. Discussion started: 27 April 2026

et al. (2005). Thanks to its design and built-in data correction algorithm, the MAAP instrument is considered one of the reference methods to measure the aerosol absorption coefficient, so that other techniques are usually corrected using MAAP observations as reference (e.g. Zanatta et al., 2016; (Renzi et al., 2025). While some recent studies questioned the reliability reliability of the MAAP as a reference method (Kalbermatter et al., 2022a; Yus-Díez et al., 2025), other studies, have reported smaller discrepancies (Romshoo et al., 2022; Heuser et al., 2025). Despite these limitations, the MAAP remains one of the most widely used instruments to quantify the aerosol absorption coefficient and eBC in monitoring stations (Savadkoohi et al., 2024), intense field observations (Yuan et al., 2021) and laboratory/chamber experiments (Kalbermatter et al., 2022b). Considering the long and diffused use of the instrument by the aerosol community, the instrument was object of several intercomparison and its operativity fully verified (Müller et al., 2011; Asmi et al., 2021; Kalbermatter et al., 2022b). The MAAP was operated continuously at CMN since May 2007, sampling air through the various inlet systems as shown in Table 1. Despite the change of the inlet, the MAAP instrument was connected to the flow splitter (in parallel to the various models of the nephelometer) with a conductive tubing having an inner diameter of ¾ inch and a length below 1 meter for the entire duration of the measuring period.

3.2 Aerosol sampling

3.2.1 Inlet system

In this part of the work, we describe the characteristics of the aerosol inlet and the conditions in the sampling line relevant for the MAAP measurements at CMN since 2007. Over 20 years, the inlet design of CMN evolved from a basic inlet to a sophisticated system with autonomous flow and temperature control and subsequent data acquisition following the recent ACTRIS-RI general recommendations for aerosol sampling. Detailed ACTRIS/GAW recommendations on atmospheric sampling may be found at https://www.actris-ecac.eu/actris-gaw-recommendation-documents.html (last accessed 11/12/2025). A whole-air-inlet (WAI) must be used, if the observatory is more than 10% of the time in cloud or fog. Considering the almost permanent occurrence of clouds at CMN across the full year (Figure S2), a WAI has been operative since 2007. Three different inlet systems have been used at the CMN observatory to sample aerosol particles since 2002 (Table 1). A simple "downward looking" inlet was used at CMN from 2002 to 5 September 2007. This inlet did not have a defined size-cut, temperature-control system or a main flow-control system. The flow at the inlet tip was of approximately 20 L min^{-1} as estimated from the sampling flow of the various aerosol measuring instruments operated from 2002 to 2007. The MAAP instrument sampled air behind the "downward looking" inlet for 247 days, accounting for approximately 4% of the full dataset. During the remaining time, absorption and eBC were quantified behind a WAI. Between September and October 2007, the downward-inlet was replaced with a WAI (WAI-1) composed of a total size particle sampling heated head. The stainless steel head was suspended 3 m above the terrace of the observatory (5.5 m from the terrain). A constant flow of 120 L min^{-1} was maintained at the inlet head using turbine ensuring laminar flow within the main stainless steel tube section having an inner diameter of 95.6 mm. Besides the heated inlet head, no additional drying system have been installed until 27 November 2022. In this date, the WAI-

https://doi.org/10.5194/essd-2026-211
Preprint. Discussion started: 27 April 2026

1 was upgraded to WAI-2 by adding: 1) a new heating-control system to prevent condensation and frost of the sampling head, 2) a dynamic flow-control system compensating the variation of total flow caused by different aerosol measurement setups and maintaining the total WAI at 150 LPM, 3) a drying system. While the outdoor geometry of the inlet remained unaltered, the main indoor line was split into 5 secondary lines connecting the aerosol instrumentation to the main inlet flow. Each line was equipped with an active drying system (model MD-700-24F, Perma pure), after which, pressure, temperature and relative were measured. Additional temperature, relative humidity and pressure measurements were performed at flow splitter, in the inlet head and at ambient.

3.2.2 Monitoring of sampling conditions

ACTRIS-RI recommends the continuous measurement of temperature, pressure, and relative humidity inside the sampling line. Until February 2023, the CMN inlet system was not equipped with dedicated sensors inside the sampling line; hence, various model of nephelometers have been used to monitor the temperature, the relative humidity and the pressure at the end of the sampling line. Overall, three different models of integrating nephelometers were operated at CMN over the 2007-2023 period: the M9003 integrating nephelometer (Ecotech Pty Ltd, Knoxfield, Australia) from May 2007 to October 2013; the TSI3565 integrating nephelometer (TSI Inc, St. Paul, MN, USA) from February 2014 to April 2023 and the AURORA3000 integrating nephelometer (Ecotech Pty Ltd, Knoxfield, Australia) from May 2023 to present (Table 1). Since February 2023, temperature, pressure and humidity are measured directly inside the sampling line before and after the drying systems.

3.2.3 Measuring periods

Although the MAAP instrument has been continuously operated since 8 May 2007, the complete MAAP time series may be split in five periods as function of the sampling setup (Table 1):

- Period A covers 2007 till September and comprises the downward inlet and the M9003 nephelometer.
- Period B goes from October 2007 to October 2013 and comprises the WAI-1 and the M9003 nephelometer.
- Period C goes from February 2014 to November 2022 and comprises the WAI-1 and the TSI3565 nephelometer.
- Period D goes from November 2022 to April 2023 and comprises the WAI-2 and the TSI3565 nephelometer.
- Period E goes from May 2023 to present days and comprises the WAI-2 and the AURORA3000 nephelometer.

While period B and C cover multiple years, period A, D and E have a data coverage below 12 months. This separation will be used to characterize the sampling efficiency and eventual biases on eBC quantification.

Table 1 Evolution of inlet type and sensors (nephelometer models) for the measurement of temperature, relative humidity and pressure in the sampling line at CMN from 2007 to 2024.

	2007	2008	2009	2010	2011	2012	2013	2014	2015	2016	2017	2018	2019	2020	2021	2022	2023	2024
eBC MASS CONCENTRATION																		

https://doi.org/10.5194/essd-2026-211
Preprint. Discussion started: 27 April 2026

Open Access Earth System Science Data Discussions

MAAP	08-May																
INLET																	
Downward inlet	05-Sep																
Whole air inlet - 1 (102-A)	10-Oct														24-Nov		
Whole air inlet - 2 (4S)															27-Nov		
TEMPERATURE – RELATIVE HUMIDITY -PRESSURE IN THE SAMPLING LINE																	
Nephelometer M9003	08-May						22-Oct										
Nephelometer TSI3565								26-Feb								05-Apr	
Nephelometer AURORA3000																04-May	
Inlet sensors																09-Feb	
PERIOD CLASSIFICATION																	
	A	B						C							D	E	

4 Data treatment to derive aerosol absorption coefficient and equivalent black carbon mass concentration

In this part of the work, we describe the full data treatment procedure necessary to derive the aerosol absorption coefficient at a wavelength of 637 nm and its conversion to eBC mass concentration. CMN is equipped with automatic routines for QA/QC since 2018 (Naitza et al., 2020). In this section we describe the updated data validation process following the most recent ACTRIS-RI guidelines provided by the ACTRIS central facility CAIS-ECAC (Center for Aerosol In-Situ – European Center for Aerosol Calibration and Characterization). This data reduction involves various treatment steps necessary to convert the MAAP raw data into Level 0, Level 1 and Level 2 aerosol absorption coefficient data. The quality control guidelines are available on the CAIS-ECAC website (https://www.actris-ecac.eu/particle-light-absorption.html#Guidelines ; last accesses 17/12/2025) while the description of the various levels is available on the EBAS data submission portal (https://ebas-submit.nilu.no/templates/Filter-Absorption-Photometer ; last accessed 17/12/2025).

https://doi.org/10.5194/essd-2026-211
Preprint. Discussion started: 27 April 2026

4.1 Screening of invalid data

The first data reduction step involves identifying and addressing mechanical and signal anomalies to produce eBC Level 0 data at the native temporal resolution of the MAAP (1 minute). Mechanical anomalies were primarily related to the sampling flow rate, in addition to routine filter spot changes and zeroing tests indicated by the instrument status. The standard sampling flow rate for the MAAP is 16.7 L min^{-1}. Due to increased uncertainty (Müller et al., 2011), periods with flow rates below 6 L min^{-1}were excluded. Periods with a sampling flow rate between 6 L $min^{-1}$and 8.3 L min^{-1} were considered valid but uncertain (Müller et al., 2011) only if the flow rate relative standard deviation remained below 5%, and no anomalies were detected in the filter load. Signal anomalies were identified by evaluating the variability of the raw BC mass concentration data provided by the MAAP at a 1-minute resolution. In alignment with ACTRIS guidelines, noise around or below zero is expected at a 1-minute resolution near the detection limit. However, negative values are unphysical in hourly averages and must be considered invalid. To identify these events, a "noise filter" was applied to remove data points associated with negative values in a one-hour rolling average (±30 minutes from the considered point). To further identify periods affected by high variability, a rolling 5^{th} and 95^{th} percentile (P05 and P95) was calculated within a one-hour time window (±30 minutes). Data points showing simultaneous negative P05 values and a difference between P95 and P05 exceeding 1 μg m^{-3} were flagged as divergent data and filtered out. Although this approach is suggested in the ACTRIS-RI guidelines, the thresholds implemented here are specific to CMN and its MAAP. Remaining data points were visually inspected for consistency and flagged as valid if no further anomalies were detected. The so derived MAAP Level 0 data report eBC mass concentration at a resolution of 1 minute, do not include invalid data and calibration periods, and are not adjusted to standard pressure and temperature.

https://doi.org/10.5194/essd-2026-211
Preprint. Discussion started: 27 April 2026

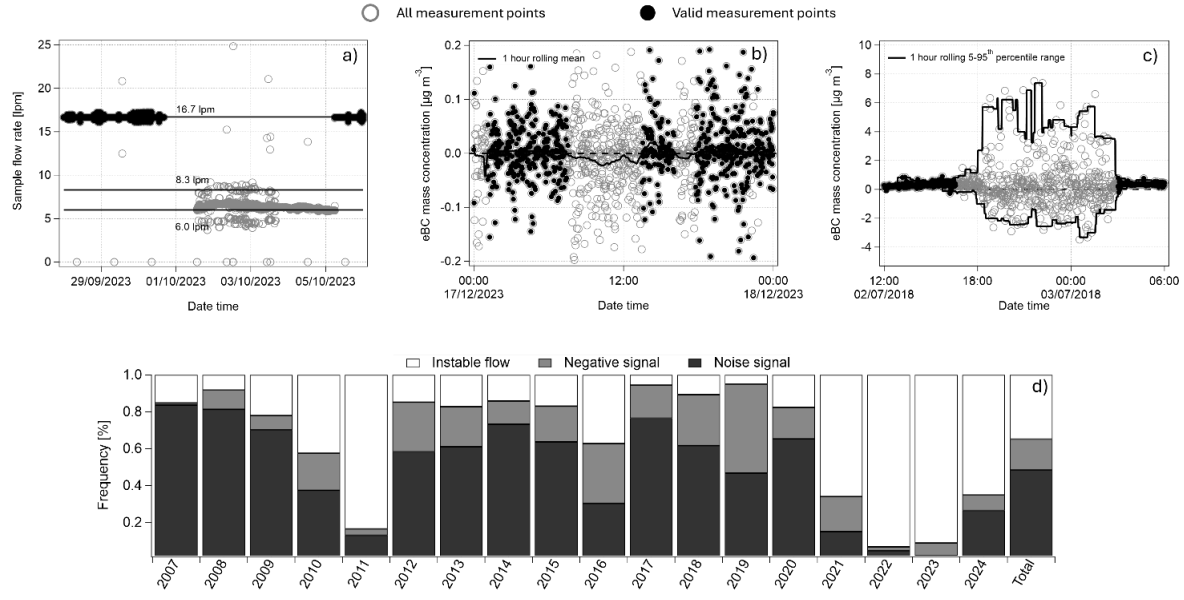

Figure 1 Overview of the flagging procedure applied to the eBC dataset. Examples of flagged data according to (a) instrumental sampling flow rate, (b) negative eBC concentrations, and (c) signal noise. Bar plot (d) reports the relative contribution of each type of irregularity to the total number of invalid data points.

4.2 Absorption coefficient correction and eBC calculation

The second step of the data reduction process aims to convert the eBC mass concentration into aerosol absorption coefficient, correct the instrumental errors and adjust the resulting atmospheric variable to standard pressure and temperature at a temporal resolution of 1 minute. The raw eBC mass concentration was converted in aerosol absorption coefficient at a wavelength of 670 nm applying the mass absorption cross-section used in the MAAP firmware (6.6 m^2 g^{-1}; Slowik et al., 2007). Being measured at an actual wavelength of 637 nm instead of a nominal wavelength of 670 nm, the aerosol absorption coefficient was adjusted with a multiplication factor of 1.05 (Müller et al., 2011). The aerosol absorption coefficient at a wavelength of 637 nm was adjusted to standard pressure (1013.25 hPa) and temperature (273.15 K) using the pressure and temperature measured in the sampling line. Starting from this Level 1 data, two additional products were extracted: aerosol absorption coefficient (Level 2) and eBC mass concentration (Level 3). Level 2 aerosol absorption coefficient is calculated as the hourly average and corresponds to the so-called "Filter Absorption Photometer Data – Level 2" publicly available on the EBAS data portal. For the present dataset, Level 1 aerosol absorption coefficient was converted in eBC mass concentration using a mass-absorption cross-section of 10 m^2 g^{-1} (Zanatta et al., 2016) at a temporal resolution of 1 minute. Level 3 eBC mass concentration was then averaged on hourly timestamp. Three valid flags were associated with the variables in the present dataset:

- Flag "000" indicates a valid data.

https://doi.org/10.5194/essd-2026-211
Preprint. Discussion started: 27 April 2026

- Flag "111" indicates an irregular data checked and accepted by data originator. It is considered valid although some irregularities were observed (e.g. sampling flow rate deviations). These irregular data points were checked manually, and their variability verified against other measurements like the Aethalometer
- Flag "640" indicates that a relative humidity higher than 40% was recorded in the sampling line. Although considered valid, these datapoints may be associated with higher noise compared to fully dry conditions.
- Flag "390" indicates valid data with an hourly data coverage below 50%. This flag is not used in the present dataset since the data coverage is specified for each hourly point.
- Flag "999" indicates invalid data and was mostly associated with mechanical problems of the instrument, high noise and background levels or a significant irregularity in the sampling flow.

4.3 Definition of uncertainties

In this section we quantify the uncertainty connected with the eBC mass concentration presented in the current dataset. The absorption coefficient measured with the MAAP and adjusted to a wavelength of 637 nm is associated with a random uncertainty of ± 15% (Zanatta et al., 2016). Besides this random error, the absorption coefficient and eBC mass concentration may be subject to errors induced by the presence of externally mixed light absorbing aerosol particles different from black carbon, the influence of relative humidity and the choice of mass absorption cross section (Table 2).

Table 2 Description of uncertainties associated with eBC quantification at the Cimone station

Source	Type	Estimation	Details
Instrumental uncertainty	Random	± 15%	Quantified by Zanatta et al. (2016)
Contribution of brown carbon to absorption	Upper estimation	+ 15%	Estimated following Rovira et al. (2025) using an absorption Ängström exponent of 1.2
	Lower estimation	+3%	Estimated following Rovira et al. (2025) using an absorption Ängström exponent of 0.8
Contribution of mineral dust to absorption	Upper estimation	+7%	Estimated from dust mass concentration using a mass absorption cross-section of 16 m^2 g^{-1} (Caponi et al., 2017). Valid only for dust days as identified by Vogel et al. (2025).
	Lower estimation	+3%	Estimated from dust mass concentration using a mass absorption cross-section of 6 m^2 g^{-1} (Caponi et al., 2017). Valid only for dust days as identified by Vogel et al. (2025).
Variability of the mass absorption cross section	Upper estimation	+30%	Estimated propagating the 1.33 geometric standard deviation associated with mass absorption cross section of ambient BC as defined in Zanatta et al. (2016)

https://doi.org/10.5194/essd-2026-211
Preprint. Discussion started: 27 April 2026

	Lower estimation	-25%	Estimated propagating the 1.33 geometric standard deviation associated with mass absorption cross section of ambient BC as defined in Zanatta et al. (2016)

4.3.1 Assumption of mass absorption cross-section

The mass absorption cross section (MAC) was used to convert the aerosol absorption coefficient to eBC mass concentration. Due to the inability of quantifying a site-specific MAC for CMN, we assumed a constant value. This assumption is crucial since MAC varies as function of combustion conditions (Corbin et al., 2019, 2022) and degree of internal mixing (Zanatta et al., 2018; Yuan et al., 2021), which, in turns, evolves as function of atmospheric conditions (Zanatta et al., 2025a) and cloud processing (Zanatta et al., 2023). Considering the seasonal variability of carbonaceous aerosol properties at CMN (Marinoni et al., 2008; Cristofanelli et al., 2013), it is fair to expect a seasonal variability of extensive optical properties as function of the season, as observed in other western Mediterranean mountain stations (Pandolfi et al., 2014; Tinorua et al., 2024). As described in Section 4.2, eBC was calculated from the aerosol absorption coefficient using a MAC value of 10 m^2 g^{-1} (Zanatta et al., 2016). This value represents the properties of internally mixed black carbon particles in background conditions being suitable for converting the aerosol absorption coefficient at background station as CMN. The geometric standard deviation (1.33) associated with the European MAC value may lead to an additional uncertainty of + 30% and -25% on the eBC mass concentration calculated at CMN.

4.3.2 Contribution to absorption of organic matter

Absorbing organic matter, also known as brown carbon (BrC), contributes to the total aerosol absorption coefficient, especially in the near UV range (e.g. Kirchstetter et al., 2004). The contribution of organic matter to the total absorption coefficient may be estimated assuming that BC is the sole aerosol absorber in the near-IR range and that its absorbing contribution follows a defined power law decay with wavelength (e.g. Yus-Díez et al., 2022). We estimated the contribution to absorption of BrC at CMN for the 2020-2024 period using multi-wavelength measurement of the aerosol absorption coefficient performed with 7-wavelength aethalometer (Model AE33 Magee Scientific; Drinovec et al., 2015). First, the absorption coefficient was adjusted at 637 nm to match the MAAP wavelength using the observed Absorption Ångström Exponent (AAE). The absorption related to BrC (Abs_{BrC}) was estimated as the difference between the total absorption and the BC absorption (Abs_{BC}). The latter was estimated by adjusting the absorption measured at 880 nm to 637 nm using a fixed AAE representative of pure BC (AAE_{BC}):

$$AbsFr_{Brc}(\lambda) = \frac{Abs_{BrC}(\lambda)}{Abs_{Tot}(\lambda)} = \frac{Abs_{Tot}(\lambda) - Abs_{BC}(\lambda)}{Abs_{Tot}(\lambda)} = \frac{Abs_{Tot}(\lambda) - Abs_{BC}(880nm)\left(\frac{880}{\lambda}\right)^{AAE_{BC}}}{Abs_{Tot}(\lambda)} \quad 1$$

More details on BrC estimation are given by Yus-Díez et al. (2022) and Rovira et al. (2025), while more detail about aethalometer observations at CMN are given in Renzi et al. (2025). To provide a range of estimations we used two different

https://doi.org/10.5194/essd-2026-211
Preprint. Discussion started: 27 April 2026

AAE_{BC} (0.8 and 1.2). Overall, the median contribution of BrC to the total aerosol absorption coefficient at 637 nm varied between 3% and 15%. This background contribution showed a clear seasonality causing higher uncertainty in the eBC concentration quantification during the winter months, compared to summer (Figure 2). This result is comparable with other locations distributed across Europe (Rovira et al., 2025). In the 590-660 nm wavelength range, in European mountain sites like CMN (e.g. Jungfraujoch, Helmos), the contribution of absorption of organic matter was 8-9%, while being slightly higher in regional background sites (8-10%).

4.3.3 Contribution to absorption of mineral dust

CMN is regularly influenced by dust transport events (Vogel et al., 2025b) and mineral dust shows a non-negligible absorption towards shorter wavelengths (Linke et al., 2006). Considering that intense dust transport events may control the aerosol absorption coefficient (Pandolfi et al., 2014; Bukowiecki et al., 2016), we investigate the potential contribution of mineral dust particle to the aerosol absorption coefficient. Days affected by dust transport events from the Sahara were identified following Duchi et al. (2016), and the dataset was separated into dust days and dust-free days.

During dust days the AAE increase, compared to dust-free days, especially towards the near-UV range, indicated enhanced absorption by non-BC particles. However, the contribution of non-BC absorbing aerosol, estimated following Section 4.3.2, remained noisy (3–21%) and showed no clear seasonal pattern. The possible internal mixing of mineral dust with organic matter prevents an unambiguous attribution of the additional absorption exclusively to dust and not BrC. Hence, we estimated the contribution of mineral dust to absorption coefficient with an alternative approach. For dust days, the dust particle concentration (PM_{Dust}) was calculated as the mass concentration of particles having a diameter larger than 1 µm (Vogel et al., 2025b). The Saharan dust absorption coefficient (Abs_{Dust}) was then calculated as the product of the dust mass concentration with the mass absorption cross-section (MAC_{Dust}). Finally, the fractional contribution of dust to the total aerosol absorption coefficient ($AbsFr_{Dust}$) was estimated as the ratio of Abs_{Dust} over total absorption:

$$AbsFr_{Dust}(\lambda) = \frac{Abs_{Dust}(\lambda)}{Abs_{Tot}(\lambda)} = \frac{PM_{Dust} * MAC_{Dust}(\lambda)}{Abs_{Tot}(\lambda)} \quad 2$$

Since optical properties of dust are highly variable, In Equation 2 we used two MAC_{Dust} representative of the North African regions. Hence, we provided a lower and upper limit of $AbsFr_{Dust}$ using 6.0 10^{-3} m^2 g^{-1} and 16 10^{-3} m^2 g^{-1} (λ=635 nm; Caponi et al., 2017). Dust contribution appeared to have a seasonal variability, reflecting the strong event frequency and intensity (Figure 2). For the current dataset, we identified 706 dust transport days (representing 14% of the eBC dataset) in which the median contribution to absorption ranged between 2.7% and 7.2%, representing one additional source of error for eBC quantification using filter-based absorption photometer. It must be considered that PM_{Dust} is based on the quantification of the total coarse PM; hence, it might contain a non-negligible mass of non-dust component, associated with the local background

https://doi.org/10.5194/essd-2026-211
Preprint. Discussion started: 27 April 2026

or sea salt aerosol particles (Marenco et al., 2006). As a consequence, the $AbsFr_{Dust}$ presented here describes an upper limit of uncertainty introduced by Saharan dust events at CMN.

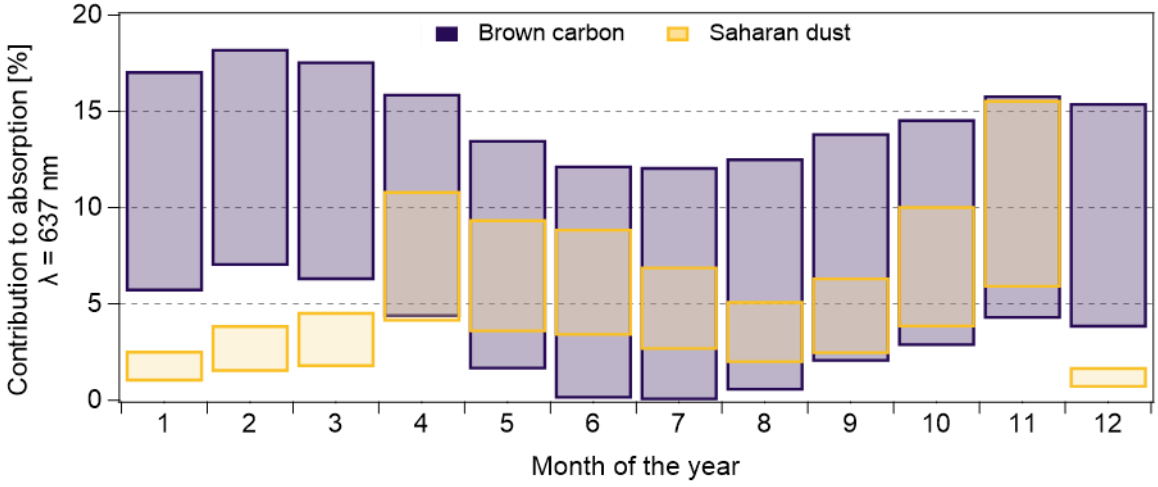

Figure 2 Estimated seasonal contribution to the aerosol absorption coefficient (wavelength = 637 nm) for brown carbon (2020-2024) and Saharan dust (2007-2024) particles. The bar width represents the range of absorption contribution considering the a MAC range for dust particles between 6.0 10-3 m^2 g^{-1} and 16 10-3 m^2 g^{-1}, and a AAE range for BC between 0.8 and 1.2.

4.1 Sampling line drying efficiency

Sampling bias may occur due to water condensation in the sampling lines and the hygroscopic growth of hydrophilic particles. Additionally, filter-based absorption photometers are sensitive to relative humidity, leading to overestimation at RH >40% (Arnott et al., 2003). We thus addressed the variability of the conditions inside the sampling line as a function of the various setups and compared it with atmospheric conditions. As discussed in more detail in Section S2 and Section S3, a permanent increase in temperature within the sampling line ensured the drying of the sampled air (Figure S3), even though the efficiency of drying strongly depends on the sampling line setup (Figure S4). Here we focus on the drying efficacy under different cloud conditions. The distributions of daily averaged RH in the sampling line for cloud-free, cloudy, liquid-cloud, and frozen-cloud days during each inlet configuration are shown in Figure 3. Overall, the presence of cloud increases the average RH in the sampling line, from 24% on cloud-free days to 31% on cloudy days. The fraction of days with mean RH above 40% is larger for liquid-cloud conditions than for frozen clouds (Figure 3a). Over the entire 2007–2024 period, only 6% of days exhibited mean RH above 40%, and these episodes are mostly associated with persistent cloud, which introduces higher uncertainty in the measurements. This uncertainty degree depends on the sampling setup. During Periods A–C (Figure 3b,c,d), indirect heating of the inlet was effective in keeping the sampled air-dry during cloud-free conditions, maintaining at least a 10 K difference between inlet temperature and ambient dew-point temperature. Under cloudy conditions, however, RH in the sampling line frequently exceeded 40%, though it remained below 60%, indicating that passive, room-temperature heating is insufficient to ensure dry sampling during sustained cloud presence. This limitation is more evident in summer, when liquid-cloud conditions and smaller ambient-to-room temperature gradients occur, and less critical in winter during freezing

https://doi.org/10.5194/essd-2026-211
Preprint. Discussion started: 27 April 2026

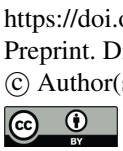

conditions. In contrast, during Periods D and E, although shorter in duration, the active drying maintained RH consistently below 30% even on liquid-cloud days and substantially reduced the variability between cloudy and cloud-free conditions (Figure 3e,f). These results demonstrate that active drying provides high repeatability and significantly reduces humidity-related uncertainty at mountain observatories.

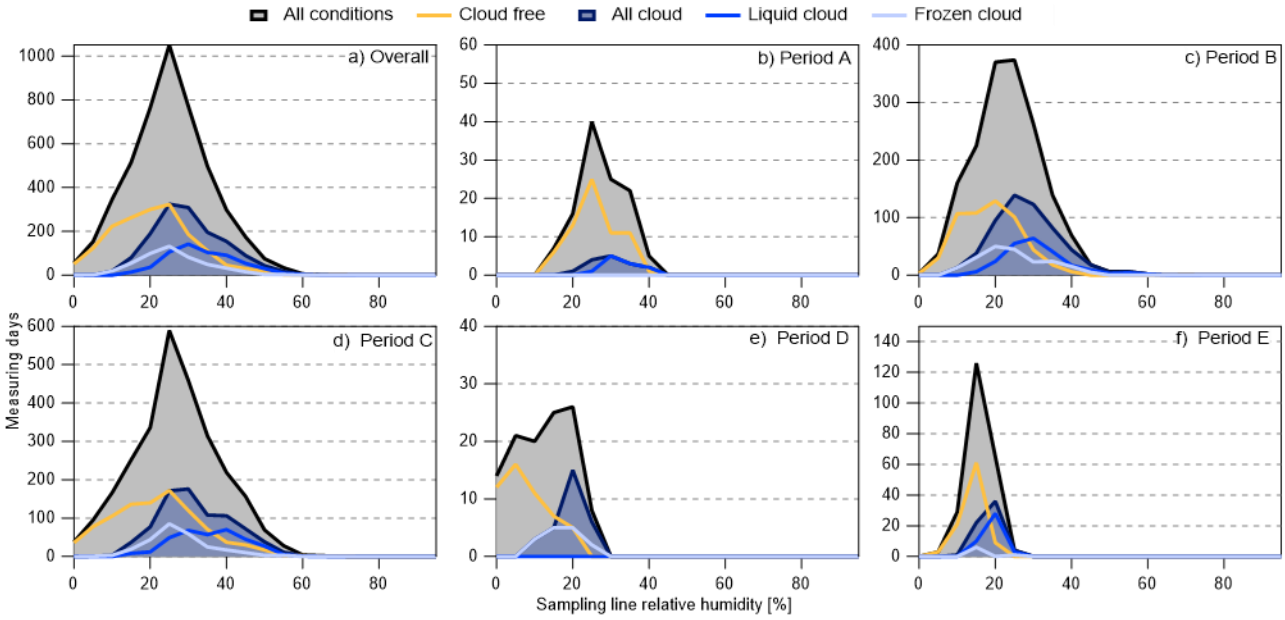

Figure 3 Histograms of the relative humidity measured in the sampling line during cloud events as function of the various configurations of the inlet line: a) overall; b) period A, downward looking inlet and M9003 nephelometer, 2007-2007; c) period B whole air inlet 1 M9003 nephelometer, 2007-2013; d) period C, whole air inlet 1 and TSI3565 nephelometer, 2014-2022; e) period D, whole air inlet 2 and TSI3565 nephelometer, 2022-2023; f) period E, whole air inlet 2 and AURORA3000 nephelometer, 2023-2024.

5 Dataset application

In this section, we describe potential applications of the dataset itself and in combination with auxiliary datasets. The objective is to demonstrate the robustness of the data and its flexibility ensured by the detailed quality assurance and high temporal resolution. We will first present a climatological application for the quantification of long-term trends; second, the integration of seasonal and dial scales processes in combination with reanalysis products; third the validation of numerical products.

5.1 Quantification of long-term trends

The number of sites measuring aerosol properties has been constantly increasing since the '90s, ensuring the availability of multi-decadal datasets worldwide (Laj et al., 2020). As emphasized by Collaud Coen et al. (2020b), multi-decadal datasets are uniquely valuable because they allow trends to be distinguished from natural variability allowing capturing changes at different temporal scales. Here, the trend analysis proposed by Collaud Coen et al. (2020a) was performed on several temporal

https://doi.org/10.5194/essd-2026-211
Preprint. Discussion started: 27 April 2026

aggregations, primarily using monthly median values. Figure 4a shows the full dataset with daily and monthly aggregations. The resulting analysis reveals a long-term decrease in eBC concentration of 55 ng m^{-3} $decade^{-1}$, consistent with reductions in mountain sites across Europe (Laj et al., 2020). Seasonal aggregation (Figure 4b) indicated that eBC trend varied across seasons, with the steepest decline in spring and almost null variation in winter. The high temporal resolution enables to calculate separately trends for summer daytime and winter nighttime periods (Figure 4c), which represents two contrasting regimes in which CMN is more representative of boundary-layer influence (summer daytime) and free-tropospheric conditions (winter nighttime). Such separation allows assessment of whether long-term trends differ under distinct atmospheric regimes and supports interpretation of processes that may not be captured in seasonally aggregated data.

https://doi.org/10.5194/essd-2026-211
Preprint. Discussion started: 27 April 2026

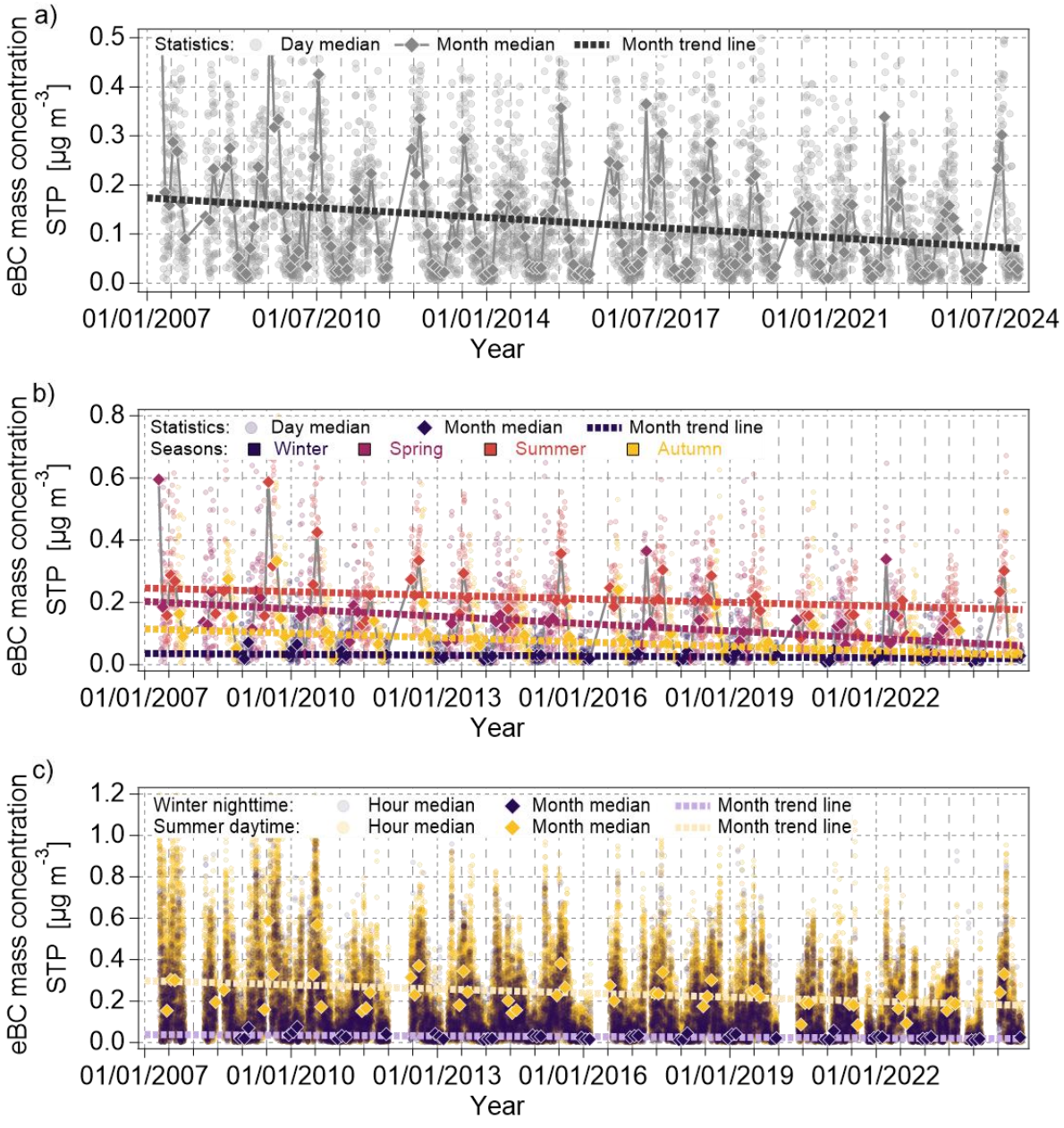

Figure 4 Time series of observed equivalent black carbon mass concentration (eBC) in the 2007-2024 period with different aggregations: a) daily and monthly time series; b) daily and monthly time series aggregated per seasons c) hourly and monthly time series aggregated per season and time of the day. Trend lines calculated on monthly median values. Seasons definition : Winter = December, January, February; Spring = March, April, May; Summer = June, July, August; Autumn = September, October, November. IQR stands for interquartile range. Time of the day definition: Daytime = 07:00-19:00; Nighttime = 12:0-04:00.

https://doi.org/10.5194/essd-2026-211
Preprint. Discussion started: 27 April 2026

5.2 Integration with reanalysis data to study local processes

Due to its altitude and regional orography, the CMN site alternates between free-tropospheric and boundary-layer conditions, with the relative contribution of each regime varying seasonally and diurnally (Collaud Coen et al., 2018; Cristofanelli et al., 2021). By using eBC concentration as a tracer for anthropogenic emissions in the planetary boundary layer (PBL), the efficiency and frequency of vertical transport from the PBL to the free troposphere can be inferred. The diel and seasonal evolution of the PBL promotes vertical export of pollution to high altitude observatories (Cristofanelli et al., 2007; Brattich et al., 2020; Tinorua et al., 2024). Even if the mesoscale PBL remains lower than the mountain site altitude, thermally driven winds are able to bring pollution along slopes up to mountainous ridges and summits (e.g. Nyeki et al., 2002; De Wekker et al., 2004). In absence of atmospheric remote sensing observations, we combined eBC observations with the PBL height available with a 0.25°x0.25° resolution within the "ERA5 hourly data on single levels" dataset (Hersbach et al., 2020) to verify the diel and seasonal vertical transport of pollution from the PBL to the mountain top. The PBL height was extracted within a grid box over the Po Valley (11.0-12.0°E; 44.5-45.0°N) on hourly averages between 2007 and 2024. This dataset represents the dynamics of the atmosphere over the nearest pollution source of CMN, allowing to address vertical transport from the surface to the free troposphere above one of the most polluted regions of Europe. A preliminary analysis aimed to define the seasonal cycle of eBC mass concentration and PBL height during daytime in the 2007-2024 period (Figure S 5). Both variables followed a clear seasonal pattern, with low concentration in winter months, when the PBL remains at its yearly minimum and higher concentration in concomitance with the maximum extent of the PBL. The high correlation (R^2=0.95) between the monthly median of eBC and the PBL height (Figure 5a) indicates that eBC concentration responds linearly to the PBL seasonal cycle. Additional analysis at higher temporal resolution considering the diel variation of eBC and PBL, which shared a similar daily cycle (Figure S 5), was performed. In contrast to the monthly aggregation, the hourly resolved data of eBC and PBL showed a not-linear relationship (Figure 5b), indicating the contribution of micro-scale processes not captured by ERA-5, the influence of local emissions or the effect of cloud and precipitation removal. Because of the extensive data coverage, anomalies or particularly intense events or deviations from a "climatological" background may be identified and addressed in more detail. The integration of additional ERA5 variables such cloud cover or large-scale precipitation can help to disentangle the contribution of changing meteorological conditions, potentially affected by climate warming, from the overall decrease in anthropogenic emissions observed in Europe. This approach could be furthermore verified with transport models acting on the removal (active and inactive scavenging) and emission (constant and varying emission) modules.

https://doi.org/10.5194/essd-2026-211
Preprint. Discussion started: 27 April 2026

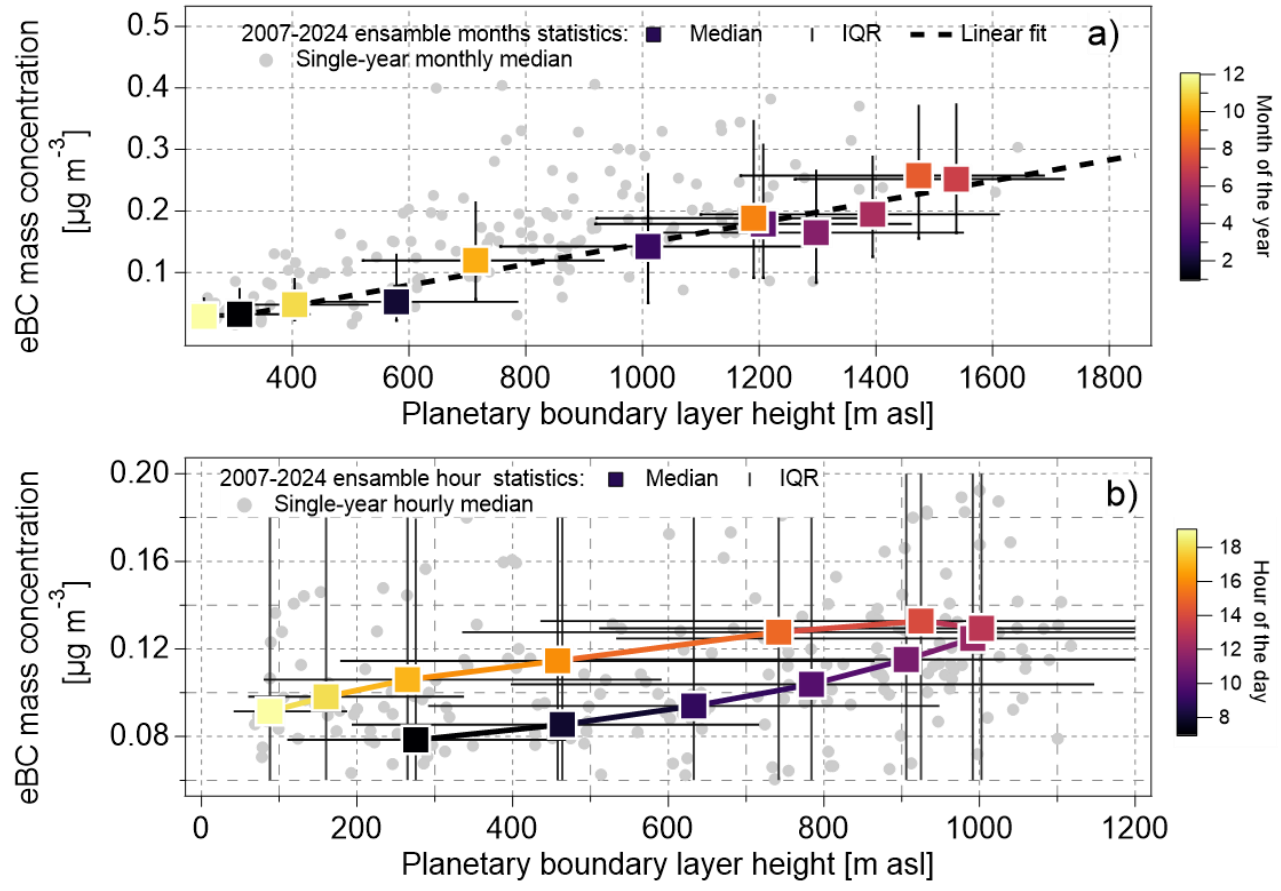

Figure 5 Correlation between daytime eBC concentration and daytime height of the planetary boundary layer: a) Correlation aggregated per months; b) Correlation aggregated for time of the day. Hourly and monthly aggregated median and interquartile range (IQR).

5.3 Comparison with numerical models

To illustrate the potential use of the CMN eBC dataset for model evaluation, we performed a comparison with FLEXPART Lagrangian particle dispersion simulations obtained within the ATMO-ACCESS program through the ACTRIS/NILU FLEXPART Request portal. While the data products are visible via graphical interface selecting the station code IT006R they are openly accessible at https://doi.org/10.82160/2cgx-5f94 (Evangeliou et al., 2025). FLEXPART (Stohl et al., 2005; Pisso et al., 2019) provides source-receptor relationships and air mass residence times that help identify the geographical and vertical origin of the air masses sampled at the station. ACTRIS FLEXPART post-processed analysis offers various products including: i) the footprint emissions sensitivity; ii) the contribution of seven anthropogenic and one natural sources; iii) the continental origin; iv) the suspension time. Although several products are available; for this specific assessment, we compared the

https://doi.org/10.5194/essd-2026-211
Preprint. Discussion started: 27 April 2026

observations of eBC with the total BC concentration estimated by FLEXPART reaching the CMN coordinates and altitude for 30 days particle tracking. More details on the whole array of FLEXPART data products are given in Section S5. The simulations cover the years 2007-2024 offering a full representativity of the observational period with a temporal resolution of 3 hours. The model–observation intercomparison presented here is not intended to provide a full attribution analysis, but rather to demonstrate how the long-term eBC record can be combined with transport modelling to assess the representativeness of simulations considering the difficulty of representing transport processes at high altitudes. We compare the FLEXPART simulations with in-situ BC observations at both high (daily) and medium (monthly) and low (yearly) temporal resolution. At daily scale, FLEXPART is able to capture short-term BC variability during pollution events, closely following the timing and magnitude of elevated concentrations (Figure S 6). On monthly scale, the model reproduces the main features of the observed seasonal cycle, including the pronounced summer maximum and winter minimum (Figure 6a). The trend analysis performed on FLEXPART data provides a decrease quantified to be -44 ng m^{-3} $decade^{-1}$, similar to observations. However, the FLEXPART estimated annual BC concentrations appear to have an almost constant positive offset centred around 0.026 µg m^{-3} (Figure 6b) with slightly positive values in winter (median = 0.051 µg m^{-3}) and negative values in summer (median = -0.017 µg m^{-3}). The weight of this offset become more evident analysing the ratio between FLEXPART and observed BC concentration (Figure 6c). While the absolute summer offset of FLEXPART appears to be minor in relative terms, the small positive overestimation in winter times leads to a considerable relative deviation in winter months, up to a factor of 13 on a single month. This simplified diagnostic highlights substantial stability of FLEXPART performances across the considered period, suggesting an accurate representation of long-term atmospheric variability. However, even small absolute offset may produce significant FLEXPART overestimation in winter months, when ambient concentrations are close to the instrumental detection limit. The long-term BC dataset presented here can therefore support detailed evaluations of model skill across temporal scales and help assess the representativeness of decadal trends and of free-tropospheric versus boundary-layer conditions.

https://doi.org/10.5194/essd-2026-211
Preprint. Discussion started: 27 April 2026

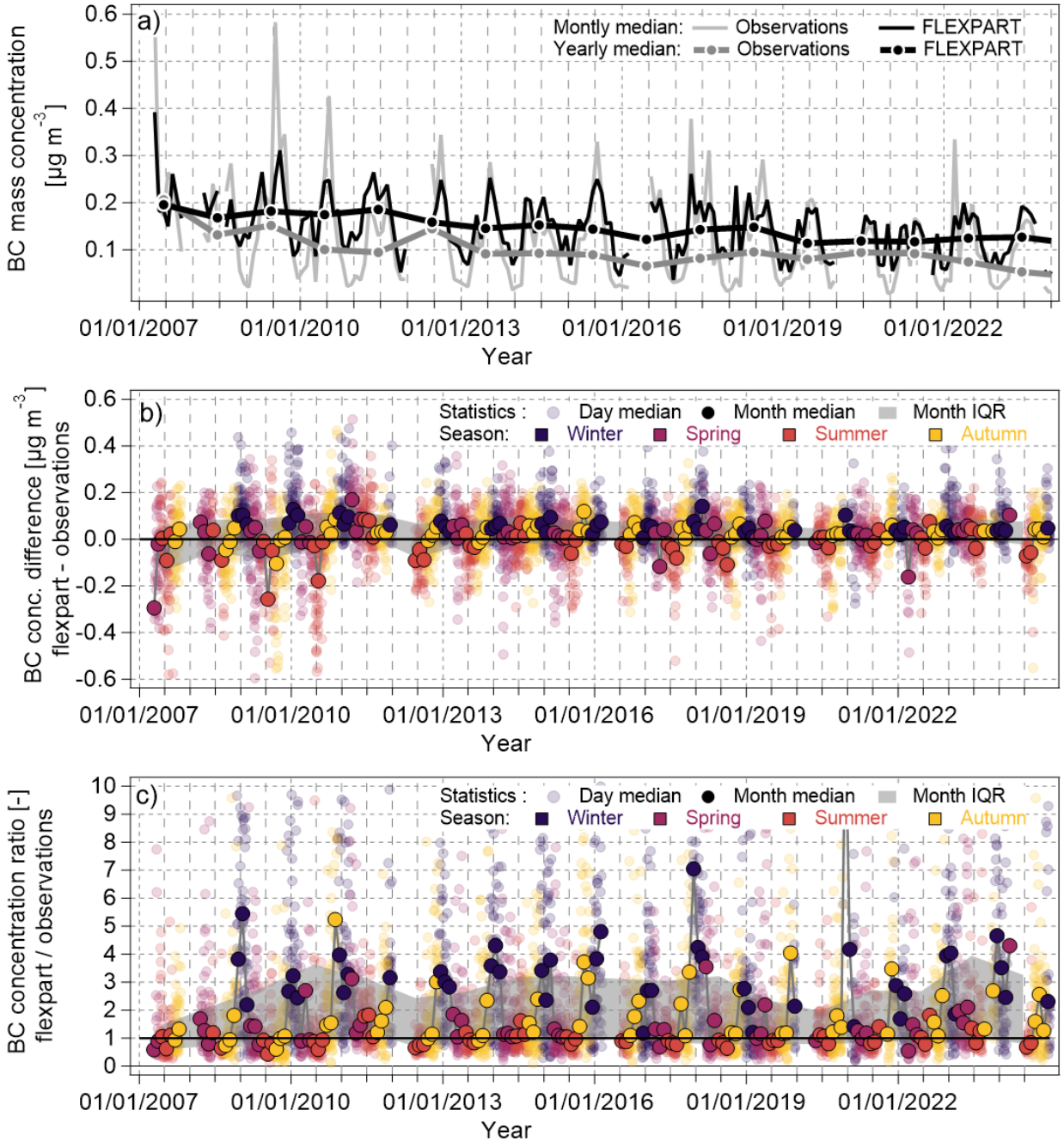

Figure 6 Comparison between eBC observations and modelled BC (FLEXPART) at CMN: a) observed and modelled median of BC mass concentration at monthly and annual resolution; b) difference between modelled BC and measured eBC mass concentration for daily and monthly median; c) Ratio between modelled BC and measured eBC for daily and monthly median. Data color-coded for seasons: Winter = December, January, February; Spring = March, April, May; Summer = June, July, August; Autumn = September, October, November. IQR stands for interquartile range.

https://doi.org/10.5194/essd-2026-211
Preprint. Discussion started: 27 April 2026

5.4 Equivalent black carbon product dataset collection over Monte Cimone, Italy 2007-2024

While the aerosol absorption coefficient (Level 2, station code IT0009R) is annually submitted to the EBAS data repository and publicly accessible at https://ebas-data.nilu.no/ (last accessed 17/12/2025), in this part of the work we present and describe the structure of the dataset named "*Equivalent black carbon product dataset collection over Monte Cimone, Italy 2007-2024*" which is publicly available on the ITINERIS-HUB data repository (https://hub.itineris.cnr.it/datasets/; last accessed 11/02/2026). The ITINERIS-HUB is an access point to the collection of data, analytics tools, services and training provided and organized by various Italian research infrastructures in the environmental scientific domain for the observation and study of processes in the atmosphere, marine domain, terrestrial biosphere, and geosphere. The dataset is organized in annual files, named "*YYYY_MAAP_eBCmassconcentration_CMN*", corresponding to one full calendar year and containing instrumental and ambient variables equally spaced in time by 1 hour. Files are provided in TXT format. Each datafile is composed by a header specifying the metadata followed by the timeseries of the variables. The metadata provides information on: i) the CMN observatory and contact persons; ii) the instrumentation, its uncertainties, and sampling conditions; iii) each of the 18 time-dependent variables, including their name, unit, and statistics. Two variables describe the starting (start_time) and ending time (end_time) of the observations, and they are calculated as the elapsed time since the midnight on the first of January (UTC). Time is here reported as fractional time where 1 hour correspond to $1/24^{th}$ of a day (0.041667). Three variables describe the condition inside the sampling line and account for pressure (int_p), temperature (int_T), and relative humidity (int_RH). Eleven variables report the concentration of equivalent black carbon mass concentration (eBC) including different statistics calculated over 1 hour. The last two rows report the fraction of valid data points for the specific hour as a fraction (DataFr), and the EBAS data flag (numflag). A full description of each time dependent variable is listed in Table 3. The dataset is paired with a PDF file named "*DatasetDescription*" providing a description of the dataset structure and the underlying data treatment.

Table 3 Description of the time dependent variables of the dataset "*Equivalent black carbon product dataset collection over Monte Cimone, Italy 2007-2024*", including their name, acronym, unit and statistics (calculated over a 1 hour time stamp).

#	Name	Acronym	Unit	Statistics
1	Start time of measurement	start_time	Fractional days	-
2	End time of measurement	end_time	Fractional days	-
3	Internal pressure	int_p	hPa	arithmetic mean
4	Internal temperature	int_T	K	arithmetic mean
5	Internal relative humidity	int_RH	%	arithmetic mean
6	eBC mass concentration	eBCmean	ug/m3	arithmetic mean

https://doi.org/10.5194/essd-2026-211
Preprint. Discussion started: 27 April 2026

7	eBC mass concentration	eBCsd	ug/m3	standard deviation
8	eBC mass concentration	eBCpc10	ug/m3	10th percentile
9	eBC mass concentration	eBCpc16	ug/m3	16th percentile
10	eBC mass concentration	eBCpc25	ug/m3	25th percentile
11	eBC mass concentration	eBCpc50	ug/m3	50th percentile
12	eBC mass concentration	eBCpc75	ug/m3	75th percentile
13	eBC mass concentration	eBCpc84	ug/m3	84th percentile
14	eBC mass concentration	eBCpc90	ug/m3	90th percentile
15	eBC mass concentration	eBCmax	ug/m3	maximum
16	eBC mass concentration	eBCmin	no unit	minimum
17	Measurement data coverage	dataFr	no unit	fraction
18	Measurement flag	numflag	no unit	

5.5 Complementary datasets

Other complementary datasets were used in the present work to evaluate the instrumental uncertainties and explore the applicability of the main eBC dataset. These datasets are produced within a wide integration of i) national project ITINERIS, ii) European research infrastructures such as ACTRIS-RI and ICOS-RI, iii) Copernicus products.

- Meteorological data since 2018 “ICOS ATC Meteo Release from Monte Cimone (8.0 m)” (Cristofanelli et al., 2025) are available on the ICOS data portal (https://hdl.handle.net/11676/-23mwxRlF7b_gqqmw3KyhAfi).
- The contribution of organic carbon to the light absorption coefficient was extracted from the wavelength-dependent optical properties of aerosol particles available as Level 2 on the EBAS data repository (https://ebas-data.nilu.no/) and referring to the station ACTRIS-RI station of “Monte Cimone”.
- The contribution of dust particles to light absorption coefficient was extracted from the dataset “Dust event identification product dataset collection over Monte Cimone, Italy 2003-2023” (Vogel et al., 2025a), publicly available on the ITINERIS-HUB data repository (https://doi.org/10.71763/xdza-fa77).
- The eBC concentration was integrated with the PBL height, which is one of the many variables composing the dataset “ERA5 hourly data on single levels from 1940 to present” (DOI: https://doi.org/10.24381/cds.adbb2d47). The dataset, described by Hersbach et al. (2020) is publicly accessible on the Copernicus Climate Data Store (https://cds.climate.copernicus.eu/).
- eBC concentration was compared with the total black carbon concentration calculated with FLEXPART. The “FLEXPART model tools for black carbon observed in Monte Cimone, Italy (IT0009R) (Evangeliou et al., 2025) includes footprint sensitivities and sector-, region-, and age-resolved source contributions to surface black carbon concentration. The data are publicly available and may be visualized with a graphical interface and are publicly available at https://doi.org/10.82160/2cgx-5f94.

https://doi.org/10.5194/essd-2026-211
Preprint. Discussion started: 27 April 2026

6 Summary and outlook

In this work we present 18 years of equivalent black carbon (eBC) mass concentration in-situ measurements at the CMN site with a filter-based absorption photometer, together with a full characterization of the data processing, associated uncertainties, and potential applications. The high temporal resolution and multi-seasonal coverage of the dataset provide a basis for investigating eBC trends, thus contributing in assessing the effectiveness of air quality and climate mitigation policies, and evaluating the influence of boundary-layer dynamics and free-tropospheric conditions on eBC variability. This dataset enables future applications such as integration with meteorological reanalyses (e.g. ERA5), validation of regional and global transport models (e.g. FLEXPART, CAMS), and assessment of aerosol perturbations linked to decadal circulation anomalies or climate variability. Given that the Mediterranean is recognized as a climate-change hotspot, sustained long-term observations such as those presented here are crucial for disentangling the impact of emission reduction policies from climatic feedback on pollutants concentration and detecting emerging perturbations. With these considerations in mind, the dataset is made openly available to support further research and to facilitate its integration into broader multi-station analyses within the ACTRIS and WMO/GAW networks.

Beyond its scientific applications, this work highlights broader structural challenges associated with maintaining long-term atmospheric observations. The operation and maintenance of the measurements, and the transmission, validation and interpretation of the data require regular investment ensuring systematic upgrading of the infrastructures and its operability which relies on specialized technical and scientific personnel. In this context, international initiatives play an important supporting role. The European research infrastructure ACTRIS promotes sustained national investments in atmospheric observation systems, while the GAW/WMO programme provides a collaborative framework and a recognized quality standard for atmospheric monitoring. Together, these initiatives contribute to strengthening the quality, coordination, and long-term sustainability of atmospheric observations.

https://doi.org/10.5194/essd-2026-211
Preprint. Discussion started: 27 April 2026

Author contribution

MZ conceived and wrote the manuscript. CP supported the PBL data processing and interpretation. FV and LR supported the absorption-interference data processing and interpretation. NE and SE supported the FLEXPART data processing and interpretation. FV supported the performed trend analysis. AM, PC, PB coordinated the observational activities at CMN. CM, LR, AM, FV, DP, PC, MZ contributed to the long-term operation of the in-situ instrumentation used in the present manuscript. All the authors contributed to the review and editing of the manuscript.

Financial support

This work was supported by the EU-funded EUSAAR PF6 (European Supersites for Atmospheric Aerosol Research), ACTRIS and ACTRIS-2 H2020 (Aerosols, Clouds and Trace gases Research InfraStructure Network), and by the Italian Ministry for University and Research (MUR) through PON PER_ACTRIS_IT, PRO-ICOS_MED and the ITINERIS projects. The Italian component of ACTRIS RI and ICOS RI were also funded on national level by Fondo Ordinario per gli Enti di ricerca (FOE) for ESFRI activities. MZ, LR and CP were funded by the ITINERIS project (no.IR0000032, D.D. no. 130/2022 – CUP B53C22002150006), funded by the EU – Next Generation EU PNRR-Mission 4 "Education and Research. FV was funded by "Progetto nazionale Rafforzamento del Capitale Umano CIR01_00015 – PER_ACTRIS_IT Potenziamento della componente italiana della Infrastruttura di Ricerca Aerosol, Clouds and Trace Gases – Rafforzamento del Capitale Umano". FLEXPART model simulations are cross-atmospheric research infrastructure services provided by ATMO-ACCESS (EU grant agreement No 101008004). The computations/simulations were performed on resources provided by Sigma2 - the National Infrastructure for High Performance Computing and Data Storage in Norway. S.E received funding from the European Union's Horizon Europe research and innovation program (101081395; EYE-CLIMA).

Code/Data availability

The main dataset named "*Equivalent black carbon product dataset collection over Monte Cimone, Italy 2007-2024*" (Zanatta et al., 2025b) is accessible on the ITINERIS-HUB data repository (https://doi.org/10.71763/itineris-hub/nfy7-yz86).
The complementary dataset named "Dust event identification product dataset collection over Monte Cimone, Italy 2003-2023" (Vogel et al., 2025a) is accessible on the ITINERIS-HUB data repository (https://doi.org/10.71763/xdza-fa77). The complementary dataset named "*FLEXPART model tools for black carbon observed in Monte Cimone, Italy (IT0009R) during 2007-2024*" (Evangeliou et al., 2025) is accessible on the NILU data repository (https://doi.org/10.82160/2cgx-5f94). The complementary dataset named "ICOS ATC Meteo Release from Monte Cimone (8.0 m)" (Cristofanelli et al., 2025) is accessible on the ICOS data repository (https://hdl.handle.net/11676/-23mwxRlF7b_gqqmw3KyhAfi).

https://doi.org/10.5194/essd-2026-211
Preprint. Discussion started: 27 April 2026

Open Access Earth System Science Data Discussions

Acknowledgements

The authors acknowledge the use of artificial intelligence tools for grammar and syntax correction of the manuscript.

https://doi.org/10.5194/essd-2026-211
Preprint. Discussion started: 27 April 2026

References

Alduchov, O. A. and Eskridge, R. E.: Improved Magnus Form Approximation of Saturation Vapor Pressure, Journal of Applied Meteorology and Climatology, 35, 601–609, https://doi.org/10.1175/1520-0450(1996)035%253C0601:IMFAOS%253E2.0.CO;2, 1996.

Ali, M. U., Siyi, L., Yousaf, B., Abbas, Q., Hameed, R., Zheng, C., Kuang, X., and Wong, M. H.: Emission sources and full spectrum of health impacts of black carbon associated polycyclic aromatic hydrocarbons (PAHs) in urban environment: A review, Critical Reviews in Environmental Science and Technology, 51, 857–896, https://doi.org/10.1080/10643389.2020.1738854, 2021.

Andrews, E., Ogren, J. A., Bonasoni, P., Marinoni, A., Cuevas, E., Rodríguez, S., Sun, J. Y., Jaffe, D. A., Fischer, E. V., Baltensperger, U., Weingartner, E., Coen, M. C., Sharma, S., Macdonald, A. M., Leaitch, W. R., Lin, N.-H., Laj, P., Arsov, T., Kalapov, I., Jefferson, A., and Sheridan, P.: Climatology of aerosol radiative properties in the free troposphere, Atmospheric Research, 102, 365–393, https://doi.org/10.1016/j.atmosres.2011.08.017, 2011.

Arnott, W. P., Moosmüller, H., Sheridan, P. J., Ogren, J. A., Raspet, R., Slaton, W. V., Hand, J. L., Kreidenweis, S. M., and Collett Jr., J. L.: Photoacoustic and filter-based ambient aerosol light absorption measurements: Instrument comparisons and the role of relative humidity, Journal of Geophysical Research: Atmospheres, 108, AAC 15-1-AAC 15-11, https://doi.org/10.1029/2002JD002165, 2003.

Asmi, A., Wiedensohler, A., Laj, P., Fjaeraa, A.-M., Sellegri, K., Birmili, W., Weingartner, E., Baltensperger, U., Zdimal, V., Zikova, N., Putaud, J.-P., Marinoni, A., Tunved, P., Hansson, H.-C., Fiebig, M., Kivekäs, N., Lihavainen, H., Asmi, E., Ulevicius, V., Aalto, P. P., Swietlicki, E., Kristensson, A., Mihalopoulos, N., Kalivitis, N., Kalapov, I., Kiss, G., de Leeuw, G., Henzing, B., Harrison, R. M., Beddows, D., O'Dowd, C., Jennings, S. G., Flentje, H., Weinhold, K., Meinhardt, F., Ries, L., and Kulmala, M.: Number size distributions and seasonality of submicron particles in Europe 2008–2009, Atmospheric Chemistry and Physics, 11, 5505–5538, https://doi.org/10.5194/acp-11-5505-2011, 2011.

Asmi, E., Backman, J., Servomaa, H., Virkkula, A., Gini, M. I., Eleftheriadis, K., Müller, T., Ohata, S., Kondo, Y., and Hyvärinen, A.: Absorption instruments inter-comparison campaign at the Arctic Pallas station, Atmospheric Measurement Techniques, 14, 5397–5413, https://doi.org/10.5194/amt-14-5397-2021, 2021.

Brattich, E., Orza, J. A. G., Cristofanelli, P., Bonasoni, P., Marinoni, A., and Tositti, L.: Advection pathways at the Mt. Cimone WMO-GAW station: Seasonality, trends, and influence on atmospheric composition, Atmospheric Environment, 234, 117513, https://doi.org/10.1016/j.atmosenv.2020.117513, 2020.

Bukowiecki, N., Weingartner, E., Gysel, M., Coen, M. C., Zieger, P., Herrmann, E., Steinbacher, M., Ga¨ggeler, H. W., and Baltensperger, U.: A Review of More than 20 Years of Aerosol Observation at the High Altitude Research Station Jungfraujoch, Switzerland (3580 m asl), Aerosol Air Qual. Res., 16, 764–788, https://doi.org/10.4209/aaqr.2015.05.0305, 2016.

Caponi, L., Formenti, P., Massabó, D., Di Biagio, C., Cazaunau, M., Pangui, E., Chevaillier, S., Landrot, G., Andreae, M. O., Kandler, K., Piketh, S., Saeed, T., Seibert, D., Williams, E., Balkanski, Y., Prati, P., and Doussin, J.-F.: Spectral- and size-resolved mass absorption efficiency of mineral dust aerosols in the shortwave spectrum: a simulation chamber study, Atmos. Chem. Phys., 17, 7175–7191, https://doi.org/10.5194/acp-17-7175-2017, 2017.

Collaud Coen, M., Andrews, E., Aliaga, D., Andrade, M., Angelov, H., Bukowiecki, N., Ealo, M., Fialho, P., Flentje, H., Hallar, A. G., Hooda, R., Kalapov, I., Krejci, R., Lin, N.-H., Marinoni, A., Ming, J., Nguyen, N. A., Pandolfi, M., Pont, V., Ries, L., Rodríguez, S., Schauer, G., Sellegri, K., Sharma, S., Sun, J., Tunved, P., Velasquez, P., and Ruffieux, D.:

https://doi.org/10.5194/essd-2026-211
Preprint. Discussion started: 27 April 2026

Identification of topographic features influencing aerosol observations at high altitude stations, Atmospheric Chemistry and Physics, 18, 12289–12313, https://doi.org/10.5194/acp-18-12289-2018, 2018.

Collaud Coen, M., Andrews, E., Bigi, A., Martucci, G., Romanens, G., Vogt, F. P. A., and Vuilleumier, L.: Effects of the prewhitening method, the time granularity, and the time segmentation on the Mann–Kendall trend detection and the associated Sen's slope, Atmospheric Measurement Techniques, 13, 6945–6964, https://doi.org/10.5194/amt-13-6945-2020, 2020a.

Collaud Coen, M., Andrews, E., Alastuey, A., Arsov, T. P., Backman, J., Brem, B. T., Bukowiecki, N., Couret, C., Eleftheriadis, K., Flentje, H., Fiebig, M., Gysel-Beer, M., Hand, J. L., Hoffer, A., Hooda, R., Hueglin, C., Joubert, W., Keywood, M., Kim, J. E., Kim, S.-W., Labuschagne, C., Lin, N.-H., Lin, Y., Lund Myhre, C., Luoma, K., Lyamani, H., Marinoni, A., Mayol-Bracero, O. L., Mihalopoulos, N., Pandolfi, M., Prats, N., Prenni, A. J., Putaud, J.-P., Ries, L., Reisen, F., Sellegri, K., Sharma, S., Sheridan, P., Sherman, J. P., Sun, J., Titos, G., Torres, E., Tuch, T., Weller, R., Wiedensohler, A., Zieger, P., and Laj, P.: Multidecadal trend analysis of in situ aerosol radiative properties around the world, Atmospheric Chemistry and Physics, 20, 8867–8908, https://doi.org/10.5194/acp-20-8867-2020, 2020b.

Corbin, J. C., Czech, H., Massabò, D., Mongeot, F. B. de, Jakobi, G., Liu, F., Lobo, P., Mennucci, C., Mensah, A. A., Orasche, J., Pieber, S. M., Prévôt, A. S. H., Stengel, B., Tay, L.-L., Zanatta, M., Zimmermann, R., Haddad, I. E., and Gysel, M.: Infrared-absorbing carbonaceous tar can dominate light absorption by marine-engine exhaust, npj Clim Atmos Sci, 2, 1–10, https://doi.org/10.1038/s41612-019-0069-5, 2019.

Corbin, J. C., Johnson, T. J., Liu, F., Sipkens, T. A., Johnson, M. P., Lobo, P., and Smallwood, G. J.: Size-dependent mass absorption cross-section of soot particles from various sources, Carbon, 192, 438–451, https://doi.org/10.1016/j.carbon.2022.02.037, 2022.

Cristofanelli, P., Bonasoni, P., Carboni, G., Calzolari, F., Casarola, L., Zauli Sajani, S., and Santaguida, R.: Anomalous high ozone concentrations recorded at a high mountain station in Italy in summer 2003, Atmospheric Environment, 41, 1383–1394, https://doi.org/10.1016/j.atmosenv.2006.10.017, 2007.

Cristofanelli, P., Marinoni, A., Arduini, J., Bonafè, U., Calzolari, F., Colombo, T., Decesari, S., Duchi, R., Facchini, M. C., Fierli, F., Finessi, E., Maione, M., Chiari, M., Calzolai, G., Messina, P., Orlandi, E., Roccato, F., and Bonasoni, P.: Significant variations of trace gas composition and aerosol properties at Mt. Cimone during air mass transport from North Africa – contributions from wildfire emissions and mineral dust, Atmospheric Chemistry and Physics, 9, 4603–4619, https://doi.org/10.5194/acp-9-4603-2009, 2009.

Cristofanelli, P., Fierli, F., Marinoni, A., Calzolari, F., Duchi, R., Burkhart, J., Stohl, A., Maione, M., Arduini, J., and Bonasoni, P.: Influence of biomass burning and anthropogenic emissions on ozone, carbon monoxide and black carbon at the Mt. Cimone GAW-WMO global station (Italy, 2165 m a.s.l.), Atmos. Chem. Phys., 13, 15–30, https://doi.org/10.5194/acp-13-15-2013, 2013.

Cristofanelli, P., Scheel, H.-E., Steinbacher, M., Saliba, M., Azzopardi, F., Ellul, R., Fröhlich, M., Tositti, L., Brattich, E., Maione, M., Calzolari, F., Duchi, R., Landi, T. C., Marinoni, A., and Bonasoni, P.: Long-term surface ozone variability at Mt. Cimone WMO/GAW global station (2165 m a.s.l., Italy), Atmospheric Environment, 101, 23–33, https://doi.org/10.1016/j.atmosenv.2014.11.012, 2015.

Cristofanelli, P., Brattich, E., Decesari, S., Landi, T. C., Maione, M., Putero, D., Tositti, L., and Bonasoni, P.: Aerosol Chemical Composition at the Mt. Cimone WMO/GAW Global Station, in: High-Mountain Atmospheric Research : The Italian Mt. Cimone WMO/GAW Global Station (2165 m a.s.l.), edited by: Cristofanelli, P., Brattich, E., Decesari, S., Landi, T. C., Maione, M., Putero, D., Tositti, L., and Bonasoni, P., Springer International Publishing, Cham, 99–118, https://doi.org/10.1007/978-3-319-61127-3_5, 2018.

https://doi.org/10.5194/essd-2026-211
Preprint. Discussion started: 27 April 2026

Cristofanelli, P., Gutiérrez, I., Adame, J. A., Bonasoni, P., Busetto, M., Calzolari, F., Putero, D., and Roccato, F.: Interannual and seasonal variability of NOx observed at the Mt. Cimone GAW/WMO global station (2165 m a.s.l., Italy), Atmospheric Environment, 249, 118245, https://doi.org/10.1016/j.atmosenv.2021.118245, 2021.

Cristofanelli, P., Trisolino, P., Calzolari, F., Busetto, M., Calidonna, C. R., Amendola, S., Arduini, J., Fratticioli, C., Hundal, R. A., Maione, M., Marcucci, F., Marinoni, A., Montaguti, S., Renzi, L., Roccato, F., Bonasoni, P., and Putero, D.: Influence of wildfire emissions to carbon dioxide (CO2) observed at the Mt. Cimone station (Italy, 2165 m asl): A multi-year investigation, Atmospheric Environment, 330, 120577, https://doi.org/10.1016/j.atmosenv.2024.120577, 2024.

Cristofanelli, P., Montaguti, S., and Trisolino, P.: ICOS ATC Meteo Release from Monte Cimone (8.0 m) | ICOS, 2025.

De Wekker, S. F. J., Steyn, D. G., and Nyeki, S.: A Comparison Of Aerosol-Layer And Convective Boundary-Layer Structure Over A Mountain Range During Staaarte '97, Boundary-Layer Meteorology, 113, 249–271, https://doi.org/10.1023/B:BOUN.0000039371.41823.37, 2004.

Duchi, R., Cristofanelli, P., Landi, T. C., Arduini, J., Bonafe', U., Bourcier, L., Busetto, M., Calzolari, F., Marinoni, A., Putero, D., and Bonasoni, P.: Long-term (2002–2012) investigation of Saharan dust transport events at Mt. Cimone GAW global station, Italy (2165 m a.s.l.), Elementa: Science of the Anthropocene, 4, 000085, https://doi.org/10.12952/journal.elementa.000085, 2016.

Evangeliou, N., Eckhardt, S., and Sollum, E.: FLEXPART model tools for black carbon observed in Monte Cimone, Italy (IT0009R) during 2007-2023 (1), https://doi.org/10.82160/2CGX-5F94, 2025.

Fuzzi, S., Baltensperger, U., Carslaw, K., Decesari, S., Denier van der Gon, H., Facchini, M. C., Fowler, D., Koren, I., Langford, B., Lohmann, U., Nemitz, E., Pandis, S., Riipinen, I., Rudich, Y., Schaap, M., Slowik, J. G., Spracklen, D. V., Vignati, E., Wild, M., Williams, M., and Gilardoni, S.: Particulate matter, air quality and climate: lessons learned and future needs, Atmos. Chem. Phys., 15, 8217–8299, https://doi.org/10.5194/acp-15-8217-2015, 2015.

Gaudel, A., Cooper, O. R., Ancellet, G., Barret, B., Boynard, A., Burrows, J. P., Clerbaux, C., Coheur, P.-F., Cuesta, J., Cuevas, E., Doniki, S., Dufour, G., Ebojie, F., Foret, G., Garcia, O., Granados-Muñoz, M. J., Hannigan, J. W., Hase, F., Hassler, B., Huang, G., Hurtmans, D., Jaffe, D., Jones, N., Kalabokas, P., Kerridge, B., Kulawik, S., Latter, B., Leblanc, T., Le Flochmoën, E., Lin, W., Liu, J., Liu, X., Mahieu, E., McClure-Begley, A., Neu, J. L., Osman, M., Palm, M., Petetin, H., Petropavlovskikh, I., Querel, R., Rahpoe, N., Rozanov, A., Schultz, M. G., Schwab, J., Siddans, R., Smale, D., Steinbacher, M., Tanimoto, H., Tarasick, D. W., Thouret, V., Thompson, A. M., Trickl, T., Weatherhead, E., Wespes, C., Worden, H. M., Vigouroux, C., Xu, X., Zeng, G., and Ziemke, J.: Tropospheric Ozone Assessment Report: Present-day distribution and trends of tropospheric ozone relevant to climate and global atmospheric chemistry model evaluation, Elementa: Science of the Anthropocene, 6, 39, https://doi.org/10.1525/elementa.291, 2018.

Giglio, L., Randerson, J. T., and van der Werf, G. R.: Analysis of daily, monthly, and annual burned area using the fourth-generation global fire emissions database (GFED4), Journal of Geophysical Research: Biogeosciences, 118, 317–328, https://doi.org/10.1002/jgrg.20042, 2013.

Heikkinen, L., Äijälä, M., Riva, M., Luoma, K., Dällenbach, K., Aalto, J., Aalto, P., Aliaga, D., Aurela, M., Keskinen, H., Makkonen, U., Rantala, P., Kulmala, M., Petäjä, T., Worsnop, D., and Ehn, M.: Long-term sub-micrometer aerosol chemical composition in the boreal forest: inter- and intra-annual variability, Atmospheric Chemistry and Physics, 20, 3151–3180, https://doi.org/10.5194/acp-20-3151-2020, 2020.

Henne, S., Brunner, D., Folini, D., Solberg, S., Klausen, J., and Buchmann, B.: Assessment of parameters describing representativeness of air quality in-situ measurement sites, Atmos. Chem. Phys., 10, 3561–3581, https://doi.org/10.5194/acp-10-3561-2010, 2010.

https://doi.org/10.5194/essd-2026-211
Preprint. Discussion started: 27 April 2026

Hersbach, H., Bell, B., Berrisford, P., Hirahara, S., Horányi, A., Muñoz-Sabater, J., Nicolas, J., Peubey, C., Radu, R., Schepers, D., Simmons, A., Soci, C., Abdalla, S., Abellan, X., Balsamo, G., Bechtold, P., Biavati, G., Bidlot, J., Bonavita, M., De Chiara, G., Dahlgren, P., Dee, D., Diamantakis, M., Dragani, R., Flemming, J., Forbes, R., Fuentes, M., Geer, A., Haimberger, L., Healy, S., Hogan, R. J., Hólm, E., Janisková, M., Keeley, S., Laloyaux, P., Lopez, P., Lupu, C., Radnoti, G., de Rosnay, P., Rozum, I., Vamborg, F., Villaume, S., and Thépaut, J.-N.: The ERA5 global reanalysis, Quarterly Journal of the Royal Meteorological Society, 146, 1999–2049, https://doi.org/10.1002/qj.3803, 2020.

Heuser, J., Di Biagio, C., Yon, J., Cazaunau, M., Bergé, A., Pangui, E., Zanatta, M., Renzi, L., Marinoni, A., Inomata, S., Yu, C., Bernardoni, V., Chevaillier, S., Ferry, D., Laj, P., Maillé, M., Massabò, D., Mazzei, F., Noyalet, G., Tanimoto, H., Temime-Roussel, B., Vecchi, R., Vernocchi, V., Formenti, P., Picquet-Varrault, B., and Doussin, J.-F.: Spectral optical properties of soot: laboratory investigation of propane flame particles and their link to composition, Atmospheric Chemistry and Physics, 25, 6407–6428, https://doi.org/10.5194/acp-25-6407-2025, 2025.

Isokääntä, S., Kim, P., Mikkonen, S., Kühn, T., Kokkola, H., Yli-Juuti, T., Heikkinen, L., Luoma, K., Petäjä, T., Kipling, Z., Partridge, D., and Virtanen, A.: The effect of clouds and precipitation on the aerosol concentrations and composition in a boreal forest environment, Atmos. Chem. Phys., 22, 11823–11843, https://doi.org/10.5194/acp-22-11823-2022, 2022.

Itahashi, S. and Uno, I.: Dramatic improvement of aerosol pollution status over the East Asian ocean: from the establishment of Japanese environmental quality standard for PM2.5 in 2009 to its achievement in 2021, Environ. Res. Lett., 19, 044065, https://doi.org/10.1088/1748-9326/ad37ce, 2024.

Jin, S., Ma, Y., Huang, Z., Huang, J., Gong, W., Liu, B., Wang, W., Fan, R., and Li, H.: A comprehensive reappraisal of long-term aerosol characteristics, trends, and variability in Asia, Atmos. Chem. Phys., 23, 8187–8210, https://doi.org/10.5194/acp-23-8187-2023, 2023.

Kalbermatter, D. M., Močnik, G., Drinovec, L., Visser, B., Röhrbein, J., Oscity, M., Weingartner, E., Hyvärinen, A.-P., and Vasilatou, K.: Comparing black-carbon- and aerosol-absorption-measuring instruments – a new system using lab-generated soot coated with controlled amounts of secondary organic matter, Atmospheric Measurement Techniques, 15, 561–572, https://doi.org/10.5194/amt-15-561-2022, 2022a.

Kalbermatter, D. M., Močnik, G., Drinovec, L., Visser, B., Röhrbein, J., Oscity, M., Weingartner, E., Hyvärinen, A.-P., and Vasilatou, K.: Comparing black-carbon- and aerosol-absorption-measuring instruments – a new system using lab-generated soot coated with controlled amounts of secondary organic matter, Atmospheric Measurement Techniques, 15, 561–572, https://doi.org/10.5194/amt-15-561-2022, 2022b.

Kirchstetter, T. W., Novakov, T., and Hobbs, P. V.: Evidence that the spectral dependence of light absorption by aerosols is affected by organic carbon, J. Geophys. Res., 109, D21208, https://doi.org/10.1029/2004JD004999, 2004.

Klimont, Z., Kupiainen, K., Heyes, C., Purohit, P., Cofala, J., Rafaj, P., Borken-Kleefeld, J., and Schöpp, W.: Global anthropogenic emissions of particulate matter including black carbon, Atmospheric Chemistry and Physics, 17, 8681–8723, https://doi.org/10.5194/acp-17-8681-2017, 2017.

Kulmala, M., Lintunen, A., Lappalainen, H., Virtanen, A., Yan, C., Ezhova, E., Nieminen, T., Riipinen, I., Makkonen, R., Tamminen, J., Sundström, A.-M., Arola, A., Hansel, A., Lehtinen, K., Vesala, T., Petäjä, T., Bäck, J., Kokkonen, T., and Kerminen, V.-M.: Opinion: The strength of long-term comprehensive observations to meet multiple grand challenges in different environments and in the atmosphere, Atmospheric Chemistry and Physics, 23, 14949–14971, https://doi.org/10.5194/acp-23-14949-2023, 2023.

https://doi.org/10.5194/essd-2026-211
Preprint. Discussion started: 27 April 2026

Kurokawa, J. and Ohara, T.: Long-term historical trends in air pollutant emissions in Asia: Regional Emission inventory in ASia (REAS) version 3, Atmospheric Chemistry and Physics, 20, 12761–12793, https://doi.org/10.5194/acp-20-12761-2020, 2020.

Laj, P., Bigi, A., Rose, C., Andrews, E., Lund Myhre, C., Collaud Coen, M., Lin, Y., Wiedensohler, A., Schulz, M., Ogren, J. A., Fiebig, M., Gliß, J., Mortier, A., Pandolfi, M., Petäja, T., Kim, S.-W., Aas, W., Putaud, J.-P., Mayol-Bracero, O., Keywood, M., Labrador, L., Aalto, P., Ahlberg, E., Alados Arboledas, L., Alastuey, A., Andrade, M., Artíñano, B., Ausmeel, S., Arsov, T., Asmi, E., Backman, J., Baltensperger, U., Bastian, S., Bath, O., Beukes, J. P., Brem, B. T., Bukowiecki, N., Conil, S., Couret, C., Day, D., Dayantolis, W., Degorska, A., Eleftheriadis, K., Fetfatzis, P., Favez, O., Flentje, H., Gini, M. I., Gregorič, A., Gysel-Beer, M., Hallar, A. G., Hand, J., Hoffer, A., Hueglin, C., Hooda, R. K., Hyvärinen, A., Kalapov, I., Kalivitis, N., Kasper-Giebl, A., Kim, J. E., Kouvarakis, G., Kranjc, I., Krejci, R., Kulmala, M., Labuschagne, C., Lee, H.-J., Lihavainen, H., Lin, N.-H., Löschau, G., Luoma, K., Marinoni, A., Martins Dos Santos, S., Meinhardt, F., Merkel, M., Metzger, J.-M., Mihalopoulos, N., Nguyen, N. A., Ondracek, J., Pérez, N., Perrone, M. R., Petit, J.-E., Picard, D., Pichon, J.-M., Pont, V., Prats, N., Prenni, A., Reisen, F., Romano, S., Sellegri, K., Sharma, S., Schauer, G., Sheridan, P., Sherman, J. P., Schütze, M., Schwerin, A., Sohmer, R., Sorribas, M., Steinbacher, M., Sun, J., Titos, G., et al.: A global analysis of climate-relevant aerosol properties retrieved from the network of Global Atmosphere Watch (GAW) near-surface observatories, Atmospheric Measurement Techniques, 13, 4353–4392, https://doi.org/10.5194/amt-13-4353-2020, 2020.

Laj, P., Myhre, C. L., Riffault, V., Amiridis, V., Fuchs, H., Eleftheriadis, K., Petäjä, T., Salameh, T., Kivekäs, N., Juurola, E., Saponaro, G., Philippin, S., Cornacchia, C., Arboledas, L. A., Baars, H., Claude, A., Mazière, M. D., Dils, B., Dufresne, M., Evangeliou, N., Favez, O., Fiebig, M., Haeffelin, M., Herrmann, H., Höhler, K., Illmann, N., Kreuter, A., Ludewig, E., Marinou, E., Möhler, O., Mona, L., Murberg, L. E., Nicolae, D., Novelli, A., O'Connor, E., Ohneiser, K., Altieri, R. M. P., Picquet-Varrault, B., Pinxteren, D. van, Pospichal, B., Putaud, J.-P., Reimann, S., Siomos, N., Stachlewska, I., Tillmann, R., Voudouri, K. A., Wandinger, U., Wiedensohler, A., Apituley, A., Comerón, A., Gysel-Beer, M., Mihalopoulos, N., Nikolova, N., Pietruczuk, A., Sauvage, S., Sciare, J., Skov, H., Svendby, T., Swietlicki, E., Tonev, D., Vaughan, G., Zdimal, V., Baltensperger, U., Doussin, J.-F., Kulmala, M., Pappalardo, G., Sundet, S. S., and Vana, M.: Aerosol, Clouds and Trace Gases Research Infrastructure (ACTRIS): The European Research Infrastructure Supporting Atmospheric Science, Bulletin of the American Meteorological Society, 105, E1098–E1136, https://doi.org/10.1175/BAMS-D-23-0064.1, 2024.

Lawrence, M. G.: The Relationship between Relative Humidity and the Dewpoint Temperature in Moist Air: A Simple Conversion and Applications, Bulletin of the American Meteorological Society, 86, 225–234, https://doi.org/10.1175/BAMS-86-2-225, 2005.

Linke, C., Mohler, O., Veres, A., Mohacsi, A., Bozoki, Z., Szabo, G., and Schnaiter, M.: Optical properties and mineralogical composition of different Saharan mineral dust samples: a laboratory study, Atmos. Chem. Phys., 2006.

Marenco, F., Bonasoni, P., Calzolari, F., Ceriani, M., Chiari, M., Cristofanelli, P., D'Alessandro, A., Fermo, P., Lucarelli, F., Mazzei, F., Nava, S., Piazzalunga, A., Prati, P., Valli, G., and Vecchi, R.: Characterization of atmospheric aerosols at Monte Cimone, Italy, during summer 2004: Source apportionment and transport mechanisms, J. Geophys. Res., 111, 2006JD007145, https://doi.org/10.1029/2006JD007145, 2006.

Marinoni, A., Cristofanelli, P., Calzolari, F., Roccato, F., Bonafè, U., and Bonasoni, P.: Continuous measurements of aerosol physical parameters at the Mt. Cimone GAW Station (2165 m asl, Italy), Science of The Total Environment, 391, 241–251, https://doi.org/10.1016/j.scitotenv.2007.10.004, 2008.

Mazzini, M., Aliaga, D., Lamphilati, J., Gysel-Beer, M., Brem, B. T., Modini, R. L., Heslin-Rees, D., Hussein, T., Zanatta, M., Cristofanelli, P., Bianchi, F., Kulmala, M., and Marinoni, A.: Aerosol Size Distribution and New Particle Formation in High Mountain Environments: A Comparative Study at Monte Cimone and Jungfraujoch GAW Stations, EGUsphere, 1–27, https://doi.org/10.5194/egusphere-2025-3842, 2025.

https://doi.org/10.5194/essd-2026-211
Preprint. Discussion started: 27 April 2026

MedECC: Climate and Environmental Change in the Mediterranean Basin – Current Situation and Risks for the Future. First Mediterranean Assessment Report, Zenodo, https://doi.org/10.5281/ZENODO.7224821, 2020.

Müller, T., Henzing, J. S., De Leeuw, G., Wiedensohler, A., Alastuey, A., Angelov, H., Bizjak, M., Collaud Coen, M., Engström, J. E., Gruening, C., Hillamo, R., Hoffer, A., Imre, K., Ivanow, P., Jennings, G., Sun, J. Y., Kalivitis, N., Karlsson, H., Komppula, M., Laj, P., Li, S.-M., Lunder, C., Marinoni, A., Martins Dos Santos, S., Moerman, M., Nowak, A., Ogren, J. A., Petzold, A., Pichon, J. M., Rodriquez, S., Sharma, S., Sheridan, P. J., Teinilä, K., Tuch, T., Viana, M., Virkkula, A., Weingartner, E., Wilhelm, R., and Wang, Y. Q.: Characterization and intercomparison of aerosol absorption photometers: result of two intercomparison workshops, Atmos. Meas. Tech., 4, 245–268, https://doi.org/10.5194/amt-4-245-2011, 2011.

Naitza, L., Cristofanelli, P., Marinoni, A., Calzolari, F., Roccato, F., Busetto, M., Sferlazzo, D., Aruffo, E., Di Carlo, P., Bencardino, M., D'Amore, F., Sprovieri, F., Pirrone, N., Dallo, F., Gabrieli, J., Vardè, M., Resci, G., Barbante, C., Bonasoni, P., and Putero, D.: Increasing the maturity of measurements of essential climate variables (ECVs) at Italian atmospheric WMO/GAW observatories by implementing automated data elaboration chains, Computers & Geosciences, 137, 104432, https://doi.org/10.1016/j.cageo.2020.104432, 2020.

Nyeki, S., Eleftheriadis, K., Baltensperger, U., Colbeck, I., Fiebig, M., Fix, A., Kiemle, C., Lazaridis, M., and Petzold, A.: Airborne Lidar and in-situ Aerosol Observations of an Elevated Layer, Leeward of the European Alps and Apennines, Geophysical Research Letters, 29, 33-1-33–4, https://doi.org/10.1029/2002GL014897, 2002.

Pandolfi, M., Ripoll, A., Querol, X., and Alastuey, A.: Climatology of aerosol optical properties and black carbon mass absorption cross section at a remote high-altitude site in the western Mediterranean Basin, Atmos. Chem. Phys., 14, 6443–6460, https://doi.org/10.5194/acp-14-6443-2014, 2014.

Pandolfi, M., Alados-Arboledas, L., Alastuey, A., Andrade, M., Angelov, C., Artiñano, B., Backman, J., Baltensperger, U., Bonasoni, P., Bukowiecki, N., Collaud Coen, M., Conil, S., Coz, E., Crenn, V., Dudoitis, V., Ealo, M., Eleftheriadis, K., Favez, O., Fetfatzis, P., Fiebig, M., Flentje, H., Ginot, P., Gysel, M., Henzing, B., Hoffer, A., Holubova Smejkalova, A., Kalapov, I., Kalivitis, N., Kouvarakis, G., Kristensson, A., Kulmala, M., Lihavainen, H., Lunder, C., Luoma, K., Lyamani, H., Marinoni, A., Mihalopoulos, N., Moerman, M., Nicolas, J., O'Dowd, C., Petäjä, T., Petit, J.-E., Pichon, J. M., Prokopciuk, N., Putaud, J.-P., Rodríguez, S., Sciare, J., Sellegri, K., Swietlicki, E., Titos, G., Tuch, T., Tunved, P., Ulevicius, V., Vaishya, A., Vana, M., Virkkula, A., Vratolis, S., Weingartner, E., Wiedensohler, A., and Laj, P.: A European aerosol phenomenology – 6: scattering properties of atmospheric aerosol particles from 28 ACTRIS sites, Atmospheric Chemistry and Physics, 18, 7877–7911, https://doi.org/10.5194/acp-18-7877-2018, 2018.

Pernov, J. B., Beddows, D., Thomas, D. C., Dall´Osto, M., Harrison, R. M., Schmale, J., Skov, H., and Massling, A.: Increased aerosol concentrations in the High Arctic attributable to changing atmospheric transport patterns, npj Clim Atmos Sci, 5, 62, https://doi.org/10.1038/s41612-022-00286-y, 2022.

Petzold, A. and Schönlinner, M.: Multi-angle absorption photometry - A new method for the measurement of aerosol light absorption and atmospheric black carbon, Journal of Aerosol Science, 35, 421–441, https://doi.org/10.1016/j.jaerosci.2003.09.005, 2004.

Petzold, A., Schloesser, H., Sheridan, P. J., Arnott, W. P., Ogren, J. A., and Virkkula, A.: Evaluation of Multiangle Absorption Photometry for Measuring Aerosol Light Absorption, Aerosol Science and Technology, 39, 40–51, https://doi.org/10.1080/027868290901945, 2005.

Petzold, A., Ogren, J. A., Fiebig, M., Laj, P., Li, S.-M., Baltensperger, U., Holzer-Popp, T., Kinne, S., Pappalardo, G., Sugimoto, N., Wehrli, C., Wiedensohler, A., and Zhang, X.-Y.: Recommendations for reporting "black carbon" measurements, Atmos. Chem. Phys., 13, 8365–8379, https://doi.org/10.5194/acp-13-8365-2013, 2013.

https://doi.org/10.5194/essd-2026-211
Preprint. Discussion started: 27 April 2026

Pisoni, E., Zauli-Sajani, S., Belis, C. A., Khomenko, S., Thunis, P., Motta, C., Van Dingenen, R., Bessagnet, B., Monforti-Ferrario, F., Maes, J., and Feyen, L.: High resolution assessment of air quality and health in Europe under different climate mitigation scenarios, Nat Commun, 16, 5134, https://doi.org/10.1038/s41467-025-60449-2, 2025.

Pisso, I., Sollum, E., Grythe, H., Kristiansen, N. I., Cassiani, M., Eckhardt, S., Arnold, D., Morton, D., Thompson, R. L., Groot Zwaaftink, C. D., Evangeliou, N., Sodemann, H., Haimberger, L., Henne, S., Brunner, D., Burkhart, J. F., Fouilloux, A., Brioude, J., Philipp, A., Seibert, P., and Stohl, A.: The Lagrangian particle dispersion model FLEXPART version 10.4, Geoscientific Model Development, 12, 4955–4997, https://doi.org/10.5194/gmd-12-4955-2019, 2019.

Putero, D., Cristofanelli, P., Chang, K.-L., Dufour, G., Beachley, G., Couret, C., Effertz, P., Jaffe, D. A., Kubistin, D., Lynch, J., Petropavlovskikh, I., Puchalski, M., Sharac, T., Sive, B. C., Steinbacher, M., Torres, C., and Cooper, O. R.: Fingerprints of the COVID-19 economic downturn and recovery on ozone anomalies at high-elevation sites in North America and western Europe, Atmospheric Chemistry and Physics, 23, 15693–15709, https://doi.org/10.5194/acp-23-15693-2023, 2023.

Renzi, L., Di Biagio, C., Heuser, J., Zanatta, M., Cazaunau, M., Bergé, A., Pangui, E., Yon, J., Isolabella, T., Massabò, D., Vernocchi, V., Mazzini, M., Yu, C., Formenti, P., Picquet-Varrault, B., Doussin, J.-F., and Marinoni, A.: The role of size in the multiple scattering correction C for dual-spot aethalometer: a field and laboratory investigation, EGUsphere, 1–26, https://doi.org/10.5194/egusphere-2025-2823, 2025.

Romshoo, B., Pöhlker, M., Wiedensohler, A., Pfeifer, S., Saturno, J., Nowak, A., Ciupek, K., Quincey, P., Vasilatou, K., Ess, M. N., Gini, M., Eleftheriadis, K., Robins, C., Gaie-Levrel, F., and Müller, T.: Importance of size representation and morphology in modelling optical properties of black carbon: comparison between laboratory measurements and model simulations, Atmospheric Measurement Techniques, 15, 6965–6989, https://doi.org/10.5194/amt-15-6965-2022, 2022.

Rovira, J., Savadkoohi, M., Chen, G. I., Močnik, G., Aas, W., Alados-Arboledas, L., Artiñano, B., Aurela, M., Backman, J., Banerji, S., Beddows, D., Brem, B., Chazeau, B., Coen, M. C., Colombi, C., Conil, S., Costabile, F., Coz, E., de Brito, J. F., Eleftheriadis, K., Favez, O., Flentje, H., Freney, E., Gregorič, A., Gysel-Beer, M., Harrison, R., Hueglin, C., Hyvärinen, A., Ivančič, M., Kalogridis, A.-C., Keernik, H., Konstantinos, G., Laj, P., Liakakou, E., Lin, C., Listrani, S., Luoma, K., Maasikmets, M., Manninen, H. E., Marchand, N., dos Santos, S. M., Mbengue, S., Mihalopoulos, N., Nicolae, D., Niemi, J. V., Norman, M., Ovadnevaite, J., Petit, J.-E., Platt, S., Prévôt, A. S. H., Pujadas, M., Putaud, J.-P., Riffault, V., Rigler, M., Rinaldi, M., Schwarz, J., Silvergren, S., Teinemaa, E., Teinilä, K., Timonen, H., Titos, G., Tobler, A., Vasilescu, J., Vratolis, S., Yttri, K. E., Yubero, E., Zíková, N., Alastuey, A., Petäjä, T., Querol, X., Yus-Díez, J., and Pandolfi, M.: A European aerosol phenomenology – 9: Light absorption properties of carbonaceous aerosol particles across surface Europe, Environment International, 195, 109185, https://doi.org/10.1016/j.envint.2024.109185, 2025.

Savadkoohi, M., Pandolfi, M., Favez, O., Putaud, J.-P., Eleftheriadis, K., Fiebig, M., Hopke, P. K., Laj, P., Wiedensohler, A., Alados-Arboledas, L., Bastian, S., Chazeau, B., María, Á. C., Colombi, C., Costabile, F., Green, D. C., Hueglin, C., Liakakou, E., Luoma, K., Listrani, S., Mihalopoulos, N., Marchand, N., Močnik, G., Niemi, J. V., Ondráček, J., Petit, J.-E., Rattigan, O. V., Reche, C., Timonen, H., Titos, G., Tremper, A. H., Vratolis, S., Vodička, P., Funes, E. Y., Zíková, N., Harrison, R. M., Petäjä, T., Alastuey, A., and Querol, X.: Recommendations for reporting equivalent black carbon (eBC) mass concentrations based on long-term pan-European in-situ observations, Environment International, 185, 108553, https://doi.org/10.1016/j.envint.2024.108553, 2024.

Slowik, J. G., Cross, E. S., Han, J.-H., Davidovits, P., Onasch, T. B., Jayne, J. T., Williams, L. R., Canagaratna, M. R., Worsnop, D. R., Chakrabarty, R. K., Moosmüller, H., Arnott, W. P., Schwarz, J. P., Gao, R.-S., Fahey, D. W., Kok, G. L., and Petzold, A.: An Inter-Comparison of Instruments Measuring Black Carbon Content of Soot Particles, Aerosol Science and Technology, 41, 295–314, https://doi.org/10.1080/02786820701197078, 2007.

Sophie Szopa, Vaishali Naik, Bhupesh Adhikary, Paulo Artaxo, Terje Berntsen, William D. Collins, Sandro Fuzzi, Laura Gallardo, Astrid Kiendler-Scharr, Zbigniew Klimont, Hong Liao, Nadine Unger, and Prodromos Zanis: Short-Lived Climate

https://doi.org/10.5194/essd-2026-211
Preprint. Discussion started: 27 April 2026

Forcers. In Climate Change 2021: The Physical Science Basis. Contribution of Working Group I to the Sixth Assessment Report of the Intergovernmental Panel on Climate Change, https://doi.org/10.1017/9781009157896, 2021.

Stohl, A., Forster, C., Frank, A., Seibert, P., and Wotawa, G.: Technical note: The Lagrangian particle dispersion model FLEXPART version 6.2, Atmospheric Chemistry and Physics, 5, 2461–2474, https://doi.org/10.5194/acp-5-2461-2005, 2005.

Tinorua, S., Denjean, C., Nabat, P., Bourrianne, T., Pont, V., Gheusi, F., and Leclerc, E.: Higher absorption enhancement of black carbon in summer shown by 2-year measurements at the high-altitude mountain site of Pic du Midi Observatory in the French Pyrenees, Atmospheric Chemistry and Physics, 24, 1801–1824, https://doi.org/10.5194/acp-24-1801-2024, 2024.

Vogel, F., Marinoni, Angela, Putero, Davide, Mona, Lucia, Ripepi, Erman, and Volini, Michele: Dust event identification product dataset collection over Monte Cimone, Italy 2003-2023, 2025a.

Vogel, F., Putero, D., Bonasoni, P., Cristofanelli, P., Zanatta, M., and Marinoni, A.: Saharan dust transport event characterization in the Mediterranean atmosphere using 21 years of in-situ observations, EGUsphere, 1–20, https://doi.org/10.5194/egusphere-2025-1278, 2025b.

WMO/GAW Report No. 227: WMO/GAW aerosol measurement procedures: guidelines and recommendations, World Meteorological Organization, Geneva, Switzerland, 2016.

Yuan, J., Modini, R. L., Zanatta, M., Herber, A. B., Müller, T., Wehner, B., Poulain, L., Tuch, T., Baltensperger, U., and Gysel-Beer, M.: Variability in the mass absorption cross section of black carbon (BC) aerosols is driven by BC internal mixing state at a central European background site (Melpitz, Germany) in winter, Atmospheric Chemistry and Physics, 21, 635–655, https://doi.org/10.5194/acp-21-635-2021, 2021.

Yus-Díez, J., Via, M., Alastuey, A., Karanasiou, A., Minguillón, M. C., Perez, N., Querol, X., Reche, C., Ivančič, M., Rigler, M., and Pandolfi, M.: Absorption enhancement of black carbon particles in a Mediterranean city and countryside: effect of particulate matter chemistry, ageing and trend analysis, Atmospheric Chemistry and Physics, 22, 8439–8456, https://doi.org/10.5194/acp-22-8439-2022, 2022.

Yus-Díez, J., Drinovec, L., Alados-Arboledas, L., Titos, G., Bazo, E., Casans, A., Patrón, D., Querol, X., Gonzalez-Romero, A., Perez García-Pando, C., and Močnik, G.: Characterization of filter photometer artifacts in soot and dust measurements – laboratory and ambient experiments using a traceably calibrated aerosol absorption reference, Atmospheric Measurement Techniques, 18, 3073–3093, https://doi.org/10.5194/amt-18-3073-2025, 2025.

Zanatta, M., Gysel, M., Bukowiecki, N., Müller, T., Weingartner, E., Areskoug, H., Fiebig, M., Yttri, K. E., Mihalopoulos, N., Kouvarakis, G., Beddows, D., Harrison, R. M., Cavalli, F., Putaud, J. P., Spindler, G., Wiedensohler, A., Alastuey, A., Pandolfi, M., Sellegri, K., Swietlicki, E., Jaffrezo, J. L., Baltensperger, U., and Laj, P.: A European aerosol phenomenology-5: Climatology of black carbon optical properties at 9 regional background sites across Europe, Atmospheric Environment, 145, 346–364, https://doi.org/10.1016/j.atmosenv.2016.09.035, 2016.

Zanatta, M., Laj, P., Gysel, M., Baltensperger, U., Vratolis, S., Eleftheriadis, K., Kondo, Y., Dubuisson, P., Winiarek, V., Kazadzis, S., Tunved, P., and Jacobi, H.-W.: Effects of mixing state on optical and radiative properties of black carbon in the European Arctic, Atmospheric Chemistry and Physics, 18, 14037–14057, https://doi.org/10.5194/acp-18-14037-2018, 2018.

Zanatta, M., Mertes, S., Jourdan, O., Dupuy, R., Järvinen, E., Schnaiter, M., Eppers, O., Schneider, J., Jurányi, Z., and Herber, A.: Airborne investigation of black carbon interaction with low-level, persistent, mixed-phase clouds in the Arctic summer, Atmospheric Chemistry and Physics, 23, 7955–7973, https://doi.org/10.5194/acp-23-7955-2023, 2023.

https://doi.org/10.5194/essd-2026-211
Preprint. Discussion started: 27 April 2026

840 Zanatta, M., Bogert, P., Ginot, P., Gong, Y., Hoshyaripour, G. A., Hu, Y., Jiang, F., Laj, P., Li, Y., Linke, C., Möhler, O., Saathoff, H., Schnaiter, M., Umo, N. S., Vogel, F., and Wagner, R.: AIDA Arctic transport experiment (part 1): simulation of northward transport and aging effect on fundamental black carbon properties, Aerosol Research Discussions, 1–33, https://doi.org/10.5194/ar-2025-12, 2025a.

Zanatta, M., Marinoni, Angela, Putero, Davide, Mona, Lucia, Ripepi, Erman, and Volini, Michele: Equivalent black carbon
845 product dataset collection over Monte Cimone, Italy 2007-2024, 2025b.